THE ASTRONOMICAL JOURNAL, 126:2867–2886, 2003 December
© 2003. The American Astronomical Society. All rights reserved. Printed in U.S.A.

THE EVOLUTION OF MASSIVE STARS. I. RED SUPERGIANTS IN THE MAGELLANIC CLOUDS

PHILIP MASSEY[1]
Lowell Observatory, 1400 West Mars Hill Road, Flagstaff, AZ 86001; Phil.Massey@lowell.edu

AND

K. A. G. OLSEN[1]
Cerro Tololo Inter-American Observatory, National Optical Astronomy Observatory, Casilla 603, La Serena, Chile; kolsen@noao.edu
Received 2003 June 4; accepted 2003 September 3

ABSTRACT

We investigate the red supergiant (RSG) content of the SMC and LMC using multiobject spectroscopy on a sample of red stars previously identified by *BVR* CCD photometry. We obtained high-accuracy (<1 km s^{-1}) radial velocities for 118 red stars seen toward the SMC and 167 red stars seen toward the LMC, confirming most of these (89% and 95%, respectively) as red supergiants. Spectral types were also determined for most of these RSGs. We find that the distribution of spectral types is skewed toward earlier type at lower metallicities: the average (median) spectral type is K5–K7 I in the SMC, M1 I in the LMC, and M2 I in the Milky Way. Our examination of the Kurucz ATLAS9 model atmospheres suggests that the effect that metallicity has on the appearance on the TiO lines is probably sufficient to account for this effect, and we argue that RSGs in the Magellanic Clouds are 100 K (LMC) and 300 K (SMC) cooler than Galactic stars of the same spectral types. The colors of the Kurucz models are not consistent with this interpretation for the SMC, although other models (e.g., Bessell et al.) show good agreement. A finer grid of higher resolution synthetic spectra appropriate to cool supergiants is needed to better determine the effective temperature scale. We compare the distribution of RSGs in the H-R diagram to that of various stellar evolutionary models; we find that none of the models produce RSGs as cool and luminous as what is actually observed. This result is much larger than any uncertainty in the effective temperature scale. We note that, were we to simply adopt the uncorrected Galactic effective scale for RSGs and apply this to our sample, then the SMC's RSGs would be underluminous compared with the LMC's, contrary to what we expect from stellar evolution considerations. In all of our H-R diagrams, however, there is an elegant sequence of decreasing effective temperatures with increasing luminosities; explaining this will be an important test of future stellar evolutionary models. Finally, we compute the blue-to-red supergiant ratio in the SMC and LMC, finding that the values are indistinguishable (∼15) for the two Clouds. We emphasize that "observed" B/R values must be carefully determined if a comparison with that predicted by stellar models is to be meaningful. The nonrotation Geneva models overestimate the number of blue to red supergiants for the SMC, but underestimate it for the LMC; however, given the inability to produce high-luminosity RSGs in the models that match what is observed in the H-R diagram, such a disagreement is not surprising.

Key words: galaxies: stellar content — galaxies: structure — Magellanic Clouds — stars: evolution — supergiants — surveys

1. INTRODUCTION

The evolution of massive stars will depend on the initial metallicity of the gas out of which they form, and thus we can expect differences in the relative numbers of various stages of massive stars among nearby galaxies. (For a comprehensive review of the subject, see Maeder & Conti 1994.) The primary effect that metallicity has is due to its influence on radiatively driven stellar winds and the resulting mass loss. Typical mass-loss rates for Galactic O-type stars are $0.5\text{–}20 \times 10^{-6}\ M_\odot\ \mathrm{yr}^{-1}$ (Puls et al. 1996), with the more massive stars losing a greater fraction of their mass during their main-sequence lifetimes.[2] A very high mass star (100 $M_\odot$) might then lose 50% of its mass during its evolution,

[1] Visiting Astronomer, Cerro Tololo Inter-American Observatory, National Optical Astronomy Observatory, which is operated by the Association of Universities for Research in Astronomy, Inc., under cooperative agreement with the National Science Foundation.

[2] Since $\dot{M}$ depends on the luminosity L as $\dot{M} \sim L^{1.7}$ (Pauldrach, Puls, & Kudritzki 1986; de Jager, Nieuwenhuijzen, & van der Hucht 1988; Kudritzki & Puls 2000), and since luminosity depends on mass M as $L \sim M^2$ for high-mass stars (Massey 1998a, using the Schaller et al. 1992 $Z = 0.02$ evolutionary tracks), we expect that the mass-loss rates will depend on the mass roughly as $\dot{M} \sim M^{3.4}$. The main-sequence lifetime τ is a relatively weak function of the mass for high-mass stars, and inspection of the Schaller et al. (1992) $Z = 0.02$ tracks suggests that $\tau_{\rm ms} \sim M^{-0.6}$. So we expect that the total mass loss during the main-sequence phase ($\Delta M = \dot{M}\tau_{\rm ms}$) will go roughly as $\Delta M \sim M^{2.8}$. Thus the fractional mass lost, $\Delta M/M$, will go as $M^{1.8}$. And, this is just on the main sequence! Stars with luminosities above $\log (L/L_\odot) \sim 5.8$ will suffer episodes of enhanced mass loss as their luminosities exceed the Eddington limit once line opacities are taken into account; this stage is likely identified with the LBV phase (stars such as η Car and S Dor) and accounts for the Humphreys & Davidson (1979) upper luminosity limit in the H-R diagram (Lamers 1997).

which has a profound effect on its path in the H-R diagram, as first shown by de Loore, De Grève, & Lamers (1977), de Loore, De Grève, & Vanbeveren (1978), Chiosi, Nasi, & Sreenivasan (1978), Chiosi, Nasi, & Bertelli (1979), Brunish & Truran (1982), and subsequent investigations. Mass-loss rates will scale with metallicity Z to some power, with the exponent variously estimated from 1.0 to 0.5 (Abbott 1982; Lamers & Cassinelli 1996; Kudritzki et al. 1989; Puls, Springmann, & Lennon 2000; Kudritzki & Puls 2000; Vink, de Koter, & Lamers 2001; Kudritzki 2002). Beyond the main sequence, mass-loss rates are highly uncertain; for instance, mass loss during the LBV phase is highly episodic and large, with little agreement in what drives the outbursts (Humphreys & Davidson 1994; Maeder & Conti 1994). Large uncertainties also exist in the mass-loss rates during the red supergiant (RSG) phase, making the subsequent tracks even less certain (Salasnich, Bressan, & Chiosi 1999). It is commonly assumed that mass-loss rates for Wolf-Rayet stars (WRs) are independent of initial metallicity, since their atmospheres have been so enriched by the products of their own nuclear burning (e.g., Schaller et al. 1992), but Crowther et al. (2002) have recently argued that iron is an important element in driving the WR winds and hence that there will be some Z dependence in their mass-loss rates.

In addition to the effects of mass loss, stellar evolutionary tracks are also sensitive to the treatments of convection and mixing (Maeder & Meynet 1987), and there is considerable disagreement among the pundits as to the proper way to include these in models (Maeder & Conti 1994). Recent emphasis has been on the role that rotation plays in mixing in massive stars (Maeder & Meynet 2000, 2002). Convection and mixing also show some dependence on metallicity (see, e.g., Meynet & Maeder 2002), and the uncertainties in their treatment underscores the fact that the physics of massive star evolution is not perfectly well understood at present.

In order to advance our understanding of massive star evolution, it is necessary to have a solid observational database with which the predictions of stellar evolutionary theory may be compared and refined. A well-known example is the relative number of blue and red supergiants, which van den Bergh (1973) first suggested varied among nearby galaxies as a result of the effects of metallicity on massive star evolution. Particularly sensitive tests include the relative numbers of different types of evolved massive stars, such as the relative number of different types of Wolf-Rayet stars (WC-type and WN-type) or the relative number of RSGs and WRs. Maeder, Lequeux, & Azzopardi (1980) proposed that the latter number ratio would be particularly sensitive to metallicity effects.

However, there are many observational difficulties in determining such statistics reliably. For Wolf-Rayet stars, there are selection effects against finding WN-type WRs (Armandroff & Massey 1985; Massey & Johnson 1998). For red supergiants, the problem is that, when we look toward a galaxy such as M31 or the Magellanic Clouds, we see not only the bona fide extragalactic RSGs but also foreground galactic red dwarfs in the same color and apparent magnitude range. Massey (1998b) found that *BVR* photometry helped separate RSGs from foreground dwarfs but was not by itself sufficient. Spectroscopy allows an accurate assessment, however. Although the luminosity indicators for late-type stars are rather subtle, an effective technique is to use the near-IR Ca II triplet lines to determine a star's radial velocity. For many Local Group galaxies this provides a very clean separation of foreground red dwarfs from extragalactic red supergiants.

Here we extend this technique to our nearest galactic neighbors, the Magellanic Clouds (MCs). Massey (2002) estimated the degree of foreground contamination would be about 10% in the appropriate magnitude/color range, far lower than the ~50% found in M31, M33, and NGC 6822 by Massey (1998b), both because the Clouds are nearer and are at higher galactic latitude. However, an accurate census of the RSG population in the Magellanic Clouds is of particular interest, as these galaxies are sufficiently close that a great deal is already known about their blue supergiant population, for which much spectroscopy has been carried out (Massey et al. 1995; Massey 2002).

Throughout this paper we will adopt the distance and average reddenings listed by van den Bergh (2000), namely, $(m-M)_0 = 18.50$ and $E(B-V) = 0.13$ for the LMC, and $(m-M)_0 = 18.85$ and $E(B-V) = 0.06$ for the SMC.

2. OBSERVATIONS AND REDUCTIONS

Our sample of red supergiant candidates comes from a recent *UBVR* CCD survey covering most of the Clouds (Massey 2002). The sample was chosen to include potential K- and M-type supergiants, based on the criteria of $(V-R)_0 > 0.6$ and a V cutoff such that $M_{\rm bol} < -7.0$ given the observed $V-R$ color and assumed average reddening (i.e., Tables 9A and 9B of Massey 2002). A few additional red stars that did not quite meet these requirements were also included.

Our spectroscopy used the Hydra fiber positioner (Barden & Ingerson 1998) on the Blanco 4 m telescope at Cerro Tololo Inter-American Observatory during the nights of (UT) 2001 October 4–6. On the first two nights grating 380 (1200 lines mm^{-1}, blaze 8000 Å) was used in first order with an RG-610 blocking filter to obtain data at the Ca II triplet lines (λλ8498, 8542, 8662). A SITe 2K × 4K CCD was used unbinned, behind a 400 mm focal length camera on a bench spectrograph, to obtain a dispersion of 0.27 Å pixel^{-1}, with a wavelength coverage extending from 8000 to 9000 Å. A 200 μm slit plate was inserted at the output of the fiber bundle to yield a resolution of 1.2 Å (4.5 pixels). On the third night (and for a small portion of an engineering night that immediately preceded the run) we used grating KPGL1 (632 lines mm^{-1}, blaze 4200 Å) in first order with no blocking filter to obtain spectra in the blue in order to determine spectral subtypes. The CCD was binned in the spectral direction by a factor of 2 to obtain a dispersion of 1.2 Å pixel^{-1}, with a wavelength coverage extending from 3900 to 6100 Å. No slit plate was used, and the resolution (set by the size of the fibers) was approximately 4 Å (3.5 binned pixels).

The Hydra fiber positioner consists of 138 fibers (300 μm, or 2\".0 in diameter) that can be accurately positioned in a 40′ diameter field of view at the RC focus of the Blanco 4 m. An atmospheric dispersion corrector is mounted above the focal plane. The closest fiber-to-fiber spacing is approximately 25″. This proved a good match to the density of RSG candidates in most of our fields.

Our observing procedure was to configure Hydra at the zenith and then obtain a short exposure of a quartz-lamp projector flat that could be used for flat fielding and for removing the relative transmissions of each fiber. (The projector flats were taken for each new configuration to guard against slight flexure changes in the CCD dewar as the liquid nitrogen cryogen evaporates.) We would then offset to the field position and align the telescope using three to seven "field orientation probes" (bundles of six closely spaced fibers) that had been placed at the coordinates of bright stars within the field; these would also be used for guiding. Our program observations then consisted of three exposures of 5 minutes in length. These would be followed by a short exposure of a comparison lamp of He, Ne, and Ar for wavelength calibration. We would then return to zenith and reconfigure for the next field. The observations were all carried out by K. A. G. O., while P. M. kibitzed from his office in Flagstaff using the internet to help examine the data in real time.

Conditions were relatively good throughout the run, with 2 hours lost at the beginning of the first night because of fog and the last hour of the third night lost to clouds. The seeing was poor on the first night ($3''$) but was significantly better ($1''$–$2''$) on subsequent nights. The variation in throughput caused by the changes in seeing have no effect on our results, as we are concerned only with the relative strengths and positions of absorption features and not on absolute spectrophotometry.

All told, we were able to obtain radial velocity information for six fields in the SMC and 10 fields in the LMC, with a repeat of one of the SMC fields on the second night as a consistency check. The same six SMC fields were observed for the purposes of spectral classification, along with seven of the LMC fields.

On our two radial velocity nights we obtained a total of 10 observations (five per night) of four radial velocity standards, spread throughout the night. Several different fibers were used for the standards, and the stars were chosen from the list of standard radial velocity (RV) stars in the 2001 Astronomical Almanac, selected for being of late-type and accessible during our run. The stars included HD 12029 (K2 III, RV = +38.6 km s^{-1}), HD 80170 (K5 III–IV, RV = 0.0 km s^{-1}), HD 213947 (K2, RV = +16.7 km s^{-1}), and HD 223311 (K4 III, RV = −20.4 km s^{-1}). As we will describe in § 3.1, there was no systematic difference from one night to the next, and our precision was sufficiently high to detect small inconsistencies in the relative velocities of the standards.

For the purposes of spectral classification, spectral standards were taken from the list of Morgan & Keenan (1973), and included HD 160371 (K2.5 Ib), HD 52005 (K3 Ib), HD 52877 (K7 Ib), HD 42475 (M0–M1 Ib), HD 42543 (M1–M2 Ia–Ib), HD 36389 (M2 Iab–Ib), HD 190788 (M3 Ib), and HD 89845 (M4.5 Ia).

After basic CCD processing (overscan bias subtraction and trimming of the data) we reduced the spectra using the IRAF DOHYDRA script. The quartz-lamp projector flats were used to define the identification, location, and shape of the fiber profiles on the chip. This information was used to "optimally extract" the program objects and comparison exposures; flat fielding and removing the fiber-to-fiber variations was done using the extracted projector flat exposures as well. We found that the illumination of the outlying fibers with the projector flat did not match the sky illumination very well. In sky-limited applications this would compromise the sky subtraction unless corrected for by observations of blank sky, say, but since our stars were quite bright compared with the sky, this made little difference in our final data. The extracted spectra were then wavelength-calibrated using the extracted comparison-line spectra. Finally, the three one-dimensional spectra of each object were averaged using bad-pixel rejection. The standard-star data were treated identically, except that a single exposure was involved, and so no averaging was done. The spectra in the red (that would be used for radial velocity measurements) were then normalized by a low-order cubic spline and then shifted by unity to make the average continuum level zero.

3. ANALYSIS

3.1. *Radial Velocities*

Radial velocities were measured by cross-correlating each Magellanic Cloud spectrum against each of the radial velocity standard-star observations. Since we could find no systematic effect in cross-correlating the spectra of the radial velocity standards from one night to the next, we simply treated all of our data the same, regardless of which night they were obtained on. We used the IRAF routine FXCOR and limited the cross-correlation to the region 8450–8700 Å in order to isolate the Ca II triplet ($\lambda\lambda$8498, 8542, 8662). The cross-correlation peaks were fitted by a parabola, resulting in an internal precision of 0.5–0.7 km s^{-1} for each measurement. The measurement based on each of the 10 standard-star observations were then averaged; the agreement between these were excellent, and the resulting means had a standard deviation of the mean of 0.2–0.3 km s^{-1}. We believe this is an honest estimate of our actual accuracy, as quite a few stars were observed twice (or even three times) owing either to their locations in overlapping fields or to two observations of the same fields on different nights. The typical agreement for these stars was 0.25 km s^{-1}. Our spectra are so well exposed, and the Ca II triplet lines so strong, that we could easily detect small systematic differences in the cross-correlations produced by different standard stars. For instance, each of the two observations of the standard star HD 213947 (obtained on separate nights) produced cross-correlations that were ~1 km s^{-1} high compared with that obtained from the ensemble, while the standard star HD 12029 produced cross-correlations that were ~1 km s^{-1} low compared with that obtained from the ensemble.[3]

Altogether, we obtained radial velocities for 118 stars in the SMC. Three were measured three times, and 42 were measured twice. For the LMC, we obtained radial velocities for 167 stars. Of these, seven were measured three times, and 35 were measured twice.

In Tables 1 and 2 we give the average radial velocities of the stars in our sample. Figure 1 shows the histograms of these velocities, with the center-of-mass systemic velocities of the Clouds indicated.

For both the SMC and LMC there is excellent agreement in the peaks of the histograms and the cataloged systemic velocities of each Cloud. The "tail" of velocities extending to lower radial velocities is readily identified as the foreground red dwarfs that we had hoped to distinguish from the members of the Clouds. For the LMC diagram the separation is quite clean. The lower systemic velocities of the SMC results in there being a little uncertainty for three stars

[3] Specifically, if we adopt the velocities of HD 213947 (16.7 km s^{-1}) and HD 223311 (−20.4 km s^{-1}) as correct, then the true radial velocity of HD 213947 is 15.0 km s^{-1} rather than the 16.7 km s^{-1} adopted by the IAU, while that of HD 12029 is 39.6 km s^{-1} rather than the 38.6 km s^{-1} adopted by the IAU.

TABLE 1

Red Stars Seen toward the SMC[a]

Star	$\alpha_{J2000.0}$	$\delta_{J2000.0}$	V	$B-V$	$V-R$	log T_{eff}[b]	M_{bol}[b]	RV[c]	Member?	Spectral Type New	Spectral Type Lit.[d]
008324	00 47 16.84	−73 08 08.4	13.08	1.64	0.85	3.565	−7.32	134.4	SMC	K0: I	
008367	00 47 18.11	−73 10 39.3	12.46	1.40	0.93	3.531	−8.58	127.9	SMC	K7 I	
008930	00 47 36.94	−73 04 44.3	12.68	2.00	1.06	3.531	−8.36	131.6	SMC	K7 I	M1 Ia
009766	00 48 01.22	−73 23 37.5	12.95	1.29	0.86	3.531	−8.09	141.6	SMC	K7 I	
010889	00 48 27.02	−73 12 12.3	12.20	2.00	1.06	3.531	−8.84	138.4	SMC	K7 I	M0 Ia
011101	00 48 31.92	−73 07 44.4	13.54	1.69	0.99	3.531	−7.50	146.4	SMC	K7 I	
011709	00 48 46.32	−73 28 20.7	12.43	1.79	0.94	3.531	−8.61	140.4	SMC	K7 I	K5–M0I
011939	00 48 51.83	−73 22 39.3	12.82	1.81	1.00	3.518	−8.59	131.8	SMC	M0 I	
012322	00 49 00.32	−72 59 35.7	12.44	1.93	1.03	3.531	−8.60	149.0	SMC	K7 I	M0 Ia
012572	00 49 05.25	−73 31 07.8	11.66	1.45	0.76	3.602	−8.35	228.5	SMC	...	
012707	00 49 08.23	−73 14 15.5	13.40	1.77	1.00	3.503	−8.52	162.6	SMC	...	
013472	00 49 24.53	−73 18 13.5	11.73	1.77	0.85	3.531	−9.31	137.6	SMC	K7: I	K0–K5I
013740	00 49 30.34	−73 26 49.9	13.47	1.77	0.96	3.531	−7.57	156.4	SMC	K7 I	
013951	00 49 34.42	−73 14 09.9	13.00	1.79	0.93	3.531	−8.04	125.0	SMC	K7 I	
015510	00 50 06.42	−73 28 11.1	12.59	1.90	0.95	3.518	−8.82	163.0	SMC	M0 I	M0 I
017656	00 50 47.22	−72 42 57.2	12.66	1.69	0.90	3.568	−7.70	134.0	SMC	K0–5 I	
018592	00 51 03.90	−72 43 17.4	11.39	1.82	0.95	3.568	−8.97	152.3	SMC	K0–2 I	K5–M0I
019551	00 51 20.23	−72 49 22.1	12.98	1.04	0.83	3.568	−7.38	145.4	SMC	K2 I	
019743	00 51 23.28	−72 38 43.8	13.45	1.67	1.05	3.544	−7.29	138.2	SMC	K5 I	M0 Iab
020133	00 51 29.68	−73 10 44.3	12.33	1.95	1.03	3.518	−9.08	170.4	SMC	M0 I	M0 Iab
020612	00 51 37.57	−72 25 59.5	12.97	1.64	0.82	3.544	−7.77	154.9	SMC	K5 I	K5–M0
023463	00 52 26.51	−72 45 15.6	12.44	1.35	0.90	3.568	−7.92	157.9	SMC	K0–5 I	
023700	00 52 30.69	−72 26 46.8	13.09	1.67	0.85	3.568	−7.27	149.8	SMC	K0–2 I	
025550	00 53 02.85	−73 07 45.9	13.35	1.67	0.94	3.568	−7.01	136.8	SMC	K2 I	
025879	00 53 08.87	−72 29 38.6	11.91	1.77	0.88	3.531	−9.13	134.5	SMC	K7 I	M0 Ia
025888	00 53 09.04	−73 04 03.6	12.08	1.82	0.95	3.538	−8.80	159.1	SMC	K5–7 I	M0 Ia−
026402	00 53 17.81	−72 46 06.9	12.78	1.05	0.75	3.568	−7.58	148.4	SMC	K0–2 I	
026778	00 53 24.56	−73 18 31.6	12.78	1.55	0.95	3.568	−7.58	153.0	SMC	K2 I	M0 Iab
027443	00 53 36.44	−73 01 34.8	12.75	1.86	1.01	3.531	−8.29	140.3	SMC	K7 I	
027945	00 53 45.74	−72 53 38.5	12.94	1.57	0.80	3.552	−7.61	135.4	SMC	K3–5 I	
030135	00 54 26.90	−72 52 59.4	12.84	1.68	0.78	3.568	−7.52	150.8	SMC	K0–2 I	
030616	00 54 35.90	−72 34 14.3	12.22	1.85	0.92	3.531	−8.82	140.4	SMC	K7 I	M0 Iab
032188	00 55 03.71	−73 00 36.6	12.40	1.75	0.86	3.544	−8.34	154.1	SMC	K5 I	
033610	00 55 26.82	−72 35 56.2	12.60	1.75	0.91	3.531	−8.44	157.4	SMC	K7 I	M0 Iab
034158	00 55 36.58	−72 36 23.6	12.79	1.78	0.95	3.531	−8.25	139.0	SMC	K7 I	K5–M0
035231	00 55 55.10	−72 40 30.4	12.02	1.32	0.66	3.568	−8.34	151.8	SMC	K2 I	
037994	00 56 43.55	−72 30 15.0	12.65	1.68	0.97	3.531	−8.39	148.6	SMC	K7 I	K5–M0
041778	00 57 56.45	−72 17 33.3	12.52	1.08	0.82	3.531	−8.52	178.9	SMC	K7 I	
042319	00 58 06.61	−72 20 59.8	13.09	1.90	0.94	3.556	−7.41	184.9	SMC	K2–5 I	
042438	00 58 08.71	−72 19 26.7	13.20	1.59	0.87	3.552	−7.35	176.5	SMC	K3–5 I	
043219	00 58 23.30	−72 48 40.7	13.06	1.84	0.94	3.518	−8.35	135.7	SMC	M0 I	M0 Iab
043725	00 58 33.21	−72 19 15.6	13.50	1.56	0.96	3.544	−7.24	182.7	SMC	K5 I	
044719	00 58 53.33	−72 08 35.3	12.98	1.53	0.82	...	...	95.4	Fgd?	K5 V?	
044724	00 58 53.54	−72 40 38.7	11.78	1.59	0.87	...	...	55.5	Fgd	Dwarf	
044763	00 58 54.44	−72 41 40.8	12.73	1.28	0.82	...	...	18.2	Fgd	Dwarf	
045378	00 59 07.16	−72 13 08.6	12.93	1.56	0.92	3.544	−7.81	179.9	SMC	K5 I	K5 I
045850	00 59 16.90	−72 25 10.9	12.88	1.76	0.87	3.568	−7.48	141.8	SMC	K0–5 I	K5–M0
046497	00 59 31.33	−72 15 46.4	12.40	1.98	0.99	3.505	−9.46	166.3	SMC	M1 I	M0 Ia−
046662	00 59 35.04	−72 04 06.2	12.90	1.88	1.07	3.491	−9.54	180.2	SMC	M2 I	M0 Ia
046910	00 59 40.58	−72 20 55.9	12.82	1.75	0.85	3.552	−7.73	160.2	SMC	K3–5 I	M0 Ia
047757	01 00 00.63	−72 19 40.2	12.52	1.87	1.02	3.505	−9.34	161.1	SMC	M1 I	K5–M0
048122	01 00 09.42	−72 08 44.5	12.19	1.78	0.89	3.556	−8.31	172.8	SMC	K3 I	
049033	01 00 30.43	−71 58 24.7	12.50	1.82	0.91	3.544	−8.24	160.2	SMC	K5 I	M0 I
049428	01 00 40.32	−72 35 58.8	12.97	1.73	0.87	3.544	−7.77	134.4	SMC	K0–7 I	K5 I
049478	01 00 41.56	−72 10 37.0	12.17	1.81	0.99	3.518	−9.24	177.1	SMC	M0 I	K5 Ia
049990	01 00 54.13	−72 51 36.3	12.20	1.66	0.85	3.544	−8.54	186.8	SMC	K5 I	K5 Ia
050237	01 01 00.31	−72 13 41.6	12.91	1.62	0.84	3.556	−7.59	179.2	SMC	K2–5 I	K5 I
050348	01 01 03.26	−72 04 39.4	12.92	1.44	0.84	3.531	−8.12	179.3	SMC	K7 I	
050360	01 01 03.58	−72 02 58.5	13.09	1.61	0.86	3.544	−7.65	163.7	SMC	K5 I	
050840	01 01 15.99	−72 13 10.0	12.57	1.95	1.02	3.499	−9.55	179.9	SMC	M1–2 I	
051000	01 01 19.92	−72 05 13.1	12.89	1.66	0.85	3.544	−7.85	177.7	SMC	K5 I	K5 I
051265	01 01 26.89	−72 01 41.3	12.87	1.51	0.86	3.552	−7.68	159.1	SMC	K3–5 I	
051694	01 01 37.77	−71 54 16.3	11.83	1.19	0.72	...	...	17.1	Fgd	G V	

TABLE 1—*Continued*

Star	$\alpha_{J2000.0}$	$\delta_{J2000.0}$	V	$B-V$	$V-R$	log T_{eff}[b]	M_{bol}[b]	RV[c]	Member?	Spectral Type New	Spectral Type Lit.[d]
051906	01 01 43.57	−72 38 25.1	13.02	1.29	0.83	3.544	−7.72	148.1	SMC	K5 I	
052334	01 01 54.16	−71 52 18.8	12.89	1.94	0.99	3.531	−8.15	165.5	SMC	K7 I	M0 Iab
052389	01 01 55.43	−72 00 29.5	12.85	1.60	0.91	3.531	−8.19	183.8	SMC	K7 I	K2 I
053557	01 02 23.71	−72 55 21.2	12.72	1.77	0.91	3.531	−8.32	170.8	SMC	K7 I	M0 I
053638	01 02 25.83	−72 38 56.9	13.16	1.83	0.89	3.544	−7.58	153.4	SMC	K2–7 I	
054111	01 02 37.22	−72 16 25.1	12.55	1.74	0.87	3.568	−7.81	153.6	SMC	K0–5 I	K5–M0
054300	01 02 42.12	−72 37 29.1	13.02	1.74	0.89	3.568	−7.34	153.8	SMC	K0–5 I	
054414	01 02 44.82	−72 01 51.9	12.93	1.65	0.85	3.552	−7.62	174.0	SMC	K3–5 I	
054708	01 02 51.37	−72 24 15.5	12.82	1.81	0.91	3.540	−8.01	136.8	SMC	K0 I	M0 Iab
055188	01 03 02.38	−72 01 52.9	14.96	2.25	1.48	3.491	−7.48	176.8	SMC	M2 I	
055275	01 03 04.34	−72 34 12.8	12.91	1.70	1.02	3.525	−8.31	212.2	SMC	K7–M0 I	K5–M0
055355	01 03 06.43	−72 28 35.1	12.45	1.86	0.95	3.525	−8.77	137.6	SMC	K7–M0 I	K5–M0
055462	01 03 08.80	−72 44 55.1	12.21	1.38	0.83	. . .	. . .	3.2	Fgd	Dwarf	
055470	01 03 08.88	−71 55 50.8	13.12	1.75	0.86	3.552	−7.43	145.1	SMC	K3–5 I	
055560	01 03 10.93	−72 18 32.9	12.96	1.66	0.90	3.552	−7.59	159.2	SMC	K3–5 I	K5–M0
055681	01 03 12.98	−72 09 26.5	12.52	1.65	0.96	3.478	−10.53	182.3	SMC	M3 I	M0–M1
055933	01 03 18.56	−72 06 46.2	12.53	0.98	0.75	3.552	−8.02	178.8	SMC	K3–5 I	
056389	01 03 27.61	−72 52 09.4	11.85	2.01	1.01	3.538	−9.03	157.0	SMC	K5–7 I	M0 I
056732	01 03 34.30	−72 06 05.8	12.86	1.53	0.94	3.531	−8.18	183.1	SMC	K7 I	
057386	01 03 47.35	−72 01 16.0	12.71	1.57	0.85	3.552	−7.84	170.3	SMC	K3–5 I	K5–M0
057472	01 03 48.89	−72 02 12.7	12.80	1.83	0.88	3.538	−8.08	175.9	SMC	K5–7 I	K5–M0
058100	01 04 01.64	−72 08 25.2	11.14	1.42	0.76	. . .	. . .	−0.3	Fgd	K2–7 V	
058149	01 04 02.77	−72 05 27.7	12.96	1.48	0.85	3.556	−7.54	177.1	SMC	K2–5 I	K5–M0
058472	01 04 09.52	−72 50 15.3	13.34	1.82	0.96	3.520	−8.02	181.8	SMC	K0 I	
058738	01 04 15.46	−72 45 19.9	12.75	1.60	0.76	3.568	−7.61	162.1	SMC	K2 I	
058839	01 04 17.71	−71 57 32.5	13.21	1.81	0.95	3.568	−7.15	192.5	SMC	K2 I	
059426	01 04 30.26	−72 04 36.1	13.08	1.80	0.99	3.538	−7.80	167.0	SMC	K5–7 I	K5–M0
059803	01 04 38.16	−72 01 27.2	11.98	1.95	0.98	3.512	−9.65	200.0	SMC	M0–1 I	
060447	01 04 53.05	−72 47 48.5	13.09	1.64	0.94	3.518	−8.32	172.6	SMC	M0 I	
061296	01 05 11.50	−72 02 27.5	13.07	1.77	0.92	3.531	−7.97	160.1	SMC	K7 I	
062427	01 05 40.04	−71 58 46.4	13.06	1.73	0.85	3.544	−7.68	170.5	SMC	K5 I	
062763	01 05 50.26	−71 58 02.2	12.12	1.20	0.72	. . .	. . .	46.3	Fgd	K V	
063114	01 06 01.37	−72 52 43.2	12.83	1.88	0.94	3.538	−8.05	194.8	SMC	K5–7 I	
063131	01 06 01.72	−72 24 03.8	12.97	1.67	0.85	3.544	−7.77	168.1	SMC	K5 I	
063188	01 06 03.21	−72 52 16.0	13.07	1.85	0.92	3.568	−7.29	175.3	SMC	K2 I	
064448	01 06 40.21	−72 28 45.2	12.68	1.55	0.76	3.544	−8.06	155.5	SMC	K2–7 I	M0 Ia–
064663	01 06 47.62	−72 16 11.9	11.87	1.40	0.88	3.531	−9.17	139.3	SMC	K7 I	
066066	01 07 29.36	−72 30 45.7	12.57	1.69	0.82	3.544	−8.17	148.6	SMC	K5 I	
066510	01 07 43.12	−72 12 15.1	11.69	1.21	0.66	. . .	. . .	−60.1	Fgd	K5 V	
066694	01 07 48.88	−72 23 42.4	12.52	1.76	0.91	3.544	−8.22	137.6	SMC	K5 I	
066754	01 07 50.91	−72 10 46.8	13.02	1.35	0.94	. . .	. . .	−40.1	Fgd	G V	
067509	01 08 13.34	−72 00 02.9	12.74	1.68	0.86	3.568	−7.62	153.2	SMC	K2 I	
067554	01 08 14.65	−72 46 40.8	12.64	1.62	0.84	3.538	−8.24	195.9	SMC	K5–7 I	
068648	01 08 52.08	−72 23 07.0	12.33	1.76	0.87	3.568	−8.03	181.4	SMC	K2 I	
069317	01 09 17.09	−72 12 42.6	12.86	1.59	1.08	. . .	. . .	13.1	Fgd	M3–4 V	
070859	01 10 19.89	−72 03 34.8	11.06	1.39	0.88	. . .	. . .	27.2	Fgd	Dwarf	
071507	01 10 50.25	−72 00 14.5	13.26	1.74	0.89	3.552	−7.29	152.7	SMC	K3–5 I	
071566	01 10 53.51	−72 25 40.0	13.00	1.76	0.89	3.531	−8.04	188.8	SMC	K7 I	
081668	01 24 54.03	−73 26 49.2	13.14	1.77	0.90	3.544	−7.60	161.3	SMC	. . .	
081961	01 25 38.80	−73 21 55.6	11.84	1.90	0.94	3.528	−9.28	160.2	SMC	. . .	
082159	01 26 09.91	−73 23 15.4	12.71	1.71	0.83	3.573	−7.60	167.2	SMC	. . .	
083202	01 29 18.52	−73 01 59.3	11.53	1.08	0.82	3.577	−8.73	158.6	SMC	. . .	
083593	01 30 33.92	−73 18 41.9	12.64	1.87	1.00	3.491	−9.80	180.1	SMC	. . .	M2 Ia
084202	01 33 08.98	−73 25 32.5	12.00	1.33	0.70	. . .	. . .	95.3	Fgd?	. . .	
084392	01 34 08.70	−73 06 04.5	11.48	1.55	1.33	. . .	. . .	−21.4	Fgd	. . .	

Note.—Units of right ascension are hours, minutes, and seconds, and units of declination are degrees, arcminutes, and arcseconds.
[a] Star indentifications, coordinates, and photometry are from Massey 2002.
[b] Based on spectral type, if available, or $V-R$ if not. See text.
[c] Radial velocity in units of kilometers per second.
[d] Literature spectral types are from Elias et al. 1985.

TABLE 2
RED STARS SEEN TOWARD THE LMC[a]

STAR	$\alpha_{J2000.0}$	$\delta_{J2000.0}$	V	$B-V$	$V-R$	log T_{eff}[b]	M_{bol}[b]	RV[c]	Member?	SPECTRAL TYPE New	SPECTRAL TYPE Lit.[d]
009392	04 50 58.71	−69 14 03.2	12.88	1.95	1.07	3.533	−7.99	263.9	LMC	. . .	
010895	04 51 30.99	−69 14 52.0	13.55	1.94	1.23	3.479	−9.31	263.2	LMC	. . .	
011656	04 51 47.29	−69 19 25.1	13.01	1.89	1.01	3.553	−7.39	276.9	LMC	. . .	
016332	04 53 14.78	−69 12 18.3	13.73	2.17	1.39	3.477	−9.22	276.8	LMC	. . .	
016554	04 53 18.50	−69 17 03.5	12.88	1.20	0.97	3.566	−7.37	267.8	LMC	. . .	
017261	04 53 30.84	−69 17 49.8	13.00	1.03	1.20	3.489	−9.39	262.1	LMC	. . .	
017338	04 53 32.34	−69 01 17.8	10.93	1.54	0.85	. . .	. . .	−13.9	Fgd	. . .	
018456	04 53 51.19	−68 50 04.3	12.57	1.60	0.98	. . .	. . .	83.0	Fgd	. . .	
021369	04 54 36.90	−69 20 22.7	11.26	1.77	0.87	3.600	−8.63	256.1	LMC	. . .	
021480	04 54 38.56	−69 11 17.4	13.19	1.82	1.48	3.477	−9.76	256.1	LMC	. . .	
021534	04 54 39.46	−69 04 36.7	12.63	2.02	1.07	3.533	−8.24	270.4	LMC	. . .	
022204	04 54 49.77	−69 30 03.0	12.72	1.98	0.99	3.560	−7.60	261.7	LMC	. . .	
023095	04 55 03.09	−69 29 13.4	14.38	2.00	1.79	3.477	−8.57	252.0	LMC	. . .	
024014	04 55 16.11	−69 19 12.8	12.82	1.47	1.23	3.479	−10.04	246.5	LMC	. . .	
024410	04 55 21.72	−69 47 17.2	14.45	2.07	1.57	3.477	−8.50	257.1	LMC	. . .	
024987	04 55 30.05	−69 29 11.1	12.08	2.04	1.09	3.526	−8.97	260.7	LMC	. . .	
025818	04 55 41.86	−69 26 24.8	11.72	2.06	1.05	3.539	−8.99	253.6	LMC	. . .	
026286	04 55 48.28	−69 24 07.1	12.37	1.96	1.04	3.543	−8.27	256.1	LMC	. . .	
028780	04 56 23.70	−69 42 11.9	12.76	1.83	0.96	3.570	−7.45	262.8	LMC	. . .	
029153	04 56 28.30	−69 40 37.6	12.85	1.79	0.98	3.563	−7.44	268.6	LMC	. . .	
030861	04 56 48.61	−69 39 55.9	12.25	1.92	1.09	3.526	−8.80	249.9	LMC	. . .	
030929	04 56 49.63	−69 48 32.0	12.06	1.64	0.73	3.647	−7.43	248.8	LMC	. . .	
035415	04 57 44.66	−69 30 35.0	13.37	1.93	1.10	3.523	−7.78	260.9	LMC	. . .	
038347	04 58 21.08	−69 33 38.3	11.30	1.35	0.73	. . .	. . .	5.1	Fgd	. . .	
054365	05 02 09.57	−70 25 02.4	13.26	1.85	1.10	3.506	−8.45	237.0	LMC	M3 I	
058820	05 03 15.36	−70 17 41.9	13.25	1.81	1.03	3.544	−7.37	251.8	LMC	M0 I	
062090	05 04 05.10	−70 22 46.7	12.50	1.96	1.00	3.531	−8.40	243.8	LMC	M1 I	
062353	05 04 09.92	−70 12 18.0	12.86	1.49	1.00	3.531	−8.04	237.2	LMC	M1 I	
064048	05 04 41.79	−70 42 37.2	13.28	1.89	1.19	3.506	−8.43	240.4	LMC	M3 I	
064706	05 04 54.13	−70 33 18.9	12.79	1.63	0.98	3.538	−7.96	238.3	LMC	M0–1 I	
065558	05 05 10.03	−70 40 03.2	12.62	1.89	1.01	3.544	−8.00	246.3	LMC	M0 I	
066778	05 05 33.44	−70 33 47.1	12.92	1.40	1.19	3.484	−9.70	240.6	LMC	M4 I	
067982	05 05 56.61	−70 35 24.0	12.76	1.93	1.09	3.477	−10.19	244.1	LMC	M4.5 I	
068098	05 05 58.92	−70 29 14.6	13.11	1.90	1.04	3.531	−7.79	240.2	LMC	M1 I	
068125	05 05 59.56	−70 48 11.4	13.43	1.83	1.20	3.484	−9.19	224.3	LMC	M4 I	M5Iab
069960	05 06 36.42	−70 32 38.7	13.10	1.91	1.02	3.518	−8.18	242.3	LMC	M2 I	
071357	05 07 05.62	−70 32 44.3	11.70	2.07	1.09	3.531	−9.20	241.8	LMC	M1 I	
072727	05 07 32.52	−70 39 04.6	13.08	2.15	1.20	3.518	−8.20	234.4	LMC	M2 I	
106201	05 17 09.11	−69 32 21.1	13.29	1.51	1.24	3.518	−7.99	261.0	LMC	M2 I	
109106	05 17 56.51	−69 40 25.4	12.96	1.85	1.02	3.518	−8.32	248.8	LMC	M2 I	
113364	05 19 03.35	−69 39 55.2	11.70	1.46	0.93	3.531	−9.20	253.0	LMC	M1 I	
116895	05 19 53.34	−69 27 33.4	12.43	1.92	1.03	3.506	−9.28	264.3	LMC	M3 I	
119219	05 20 23.69	−69 33 27.3	12.14	2.04	0.98	3.506	−9.57	259.4	LMC	M3 I	
123778	05 21 28.06	−69 30 16.5	13.49	1.78	1.10	3.506	−8.22	274.2	LMC	M3 I	
124836	05 21 43.54	−69 21 27.6	13.19	1.59	1.01	3.553	−7.21	274.6	LMC	. . .	
126683	05 22 11.01	−69 17 24.2	11.60	1.24	0.67	. . .	. . .	93.3	Fgd	K2 V	
128130	05 22 31.21	−69 34 05.1	13.07	1.86	1.00	3.518	−8.21	259.0	LMC	M2 I	
130426	05 23 02.84	−69 20 37.1	13.18	1.88	1.05	3.531	−7.72	256.4	LMC	M1 I	
131735	05 23 34.09	−69 19 07.0	12.65	1.84	0.89	3.556	−7.71	234.8	LMC	K7 I	
134383	05 25 44.95	−69 04 48.9	13.46	1.65	1.21	3.506	−8.25	268.4	LMC	M3 I	M3 I
135720	05 26 27.52	−69 10 55.5	13.57	1.85	1.35	3.506	−8.14	269.9	LMC	M3 I	
135754	05 26 28.32	−69 07 57.4	13.07	1.96	1.05	3.531	−7.83	279.0	LMC	M1 I	
136042	05 26 34.92	−68 51 40.1	12.24	1.08	1.09	3.531	−8.66	266.0	LMC	M1 I	M2 I +
136348	05 26 42.20	−68 56 38.7	13.11	1.89	1.05	3.531	−7.79	276.7	LMC	M1 I	
136378	05 26 42.79	−68 57 13.4	13.28	1.97	1.11	3.506	−8.43	301.0	LMC	M3 I	
137624	05 27 10.38	−69 16 17.6	13.16	1.88	1.02	3.544	−7.46	279.1	LMC	M0 I	
137818	05 27 14.33	−69 11 10.7	13.33	1.74	1.20	3.506	−8.38	274.9	LMC	M3 I	
138405	05 27 26.86	−69 00 02.0	13.08	1.83	1.02	3.544	−7.54	271.8	LMC	M0 I	M0 Iab
138475	05 27 28.16	−69 00 36.0	12.65	1.66	1.03	3.544	−7.97	271.0	LMC	M0 I	M1 Ia−
138552	05 27 29.84	−67 14 12.9	12.80	1.54	1.18	3.531	−8.10	296.1	LMC	. . .	M1 Ia
139027	05 27 39.72	−69 09 01.1	12.13	1.15	0.92	3.556	−8.23	281.4	LMC	K7 I	M1 Ia
139413	05 27 47.62	−69 13 20.3	12.68	1.53	1.17	3.506	−9.03	272.8	LMC	M3 I	
139588	05 27 51.22	−67 18 04.3	13.19	1.83	1.05	3.531	−7.71	292.9	LMC	M1 I	

TABLE 2—*Continued*

Star	$\alpha_{J2000.0}$	$\delta_{J2000.0}$	V	$B-V$	$V-R$	log T_{eff}[b]	M_{bol}[b]	RV[c]	Member?	Spectral Type New	Spectral Type Lit.[d]
139591	05 27 51.28	−69 10 45.8	12.54	1.40	0.96	3.525	−8.53	265.5	LMC	M1–2 I	
140006	05 28 00.12	−69 07 42.3	13.05	1.71	0.97	3.512	−8.44	267.8	LMC	M2–3 I	M0 Ia
140296	05 28 06.11	−69 07 13.5	13.12	1.87	1.18	3.525	−7.95	271.2	LMC	M1–2 I	M0 Ia
140403	05 28 08.18	−69 13 10.8	13.01	2.01	1.15	3.484	−9.61	267.7	LMC	M3–5 I	
140782	05 28 16.01	−69 12 01.1	13.00	1.67	1.03	3.531	−7.90	271.4	LMC	M1 I	
140912	05 28 18.69	−69 07 34.7	12.83	1.13	0.97	3.531	−8.07	276.4	LMC	M1 I	M1 Ia−
141377	05 28 28.01	−69 12 57.2	10.93	1.61	0.70	3.657	−8.48	272.1	LMC	K0 I	
141507	05 28 30.42	−69 00 44.7	12.98	1.90	1.01	3.544	−7.64	285.1	LMC	M0 I	
141568	05 28 31.63	−69 05 31.2	13.23	2.02	1.19	3.512	−8.26	272.5	LMC	M2–3 I	M2 Iab
142102	05 28 43.26	−67 18 28.5	12.84	1.89	0.99	3.556	−7.52	311.8	LMC	K7 I	
142202	05 28 45.59	−68 58 02.3	12.15	1.65	1.03	3.538	−8.60	272.3	LMC	M0–M1 I	M0–M1
142907	05 29 00.86	−68 46 33.6	13.05	1.89	1.06	3.531	−7.85	273.1	LMC	M1 I	
143035	05 29 03.58	−69 06 46.3	13.52	1.93	1.27	3.484	−9.10	268.3	LMC	M3–4.5	
143137	05 29 05.59	−67 18 18.0	12.79	1.11	0.91	3.544	−7.83	314.5	LMC	M0 I	M0 Iab
143280	05 29 08.49	−69 12 18.6	13.27	1.94	1.13	3.506	−8.44	269.3	LMC	M3 I	
143877	05 29 21.10	−68 47 31.5	11.82	1.94	0.95	3.556	−8.54	273.2	LMC	K7 I	M1Ia
143898	05 29 21.49	−69 00 20.3	11.96	0.55	0.76	3.525	−9.11	285.5	LMC	M1–2 I	
144217	05 29 27.66	−69 08 50.3	12.23	1.67	1.13	3.531	−8.67	267.9	LMC	M1 I	M1 Ia
145013	05 29 42.32	−68 57 17.3	12.15	1.89	1.16	3.518	−9.13	273.0	LMC	M2 I	M1Ia
145112	05 29 44.02	−69 05 50.2	12.31	2.08	1.07	3.512	−9.18	263.5	LMC	M2–3	
145716	05 29 54.85	−69 04 15.6	12.49	1.86	0.96	3.538	−8.26	285.0	LMC	M0–1	
145728	05 29 55.04	−67 18 36.9	12.45	1.19	1.02	3.506	−9.26	308.2	LMC	M3 I	M1Ia +
146126	05 30 02.36	−67 02 45.0	11.17	1.80	0.84	3.568	−9.05	314.3	LMC	K5 I	
146244	05 30 04.63	−68 47 28.9	12.92	1.92	0.98	3.556	−7.44	275.0	LMC	K7 I	M0 Iab
146266	05 30 04.99	−69 03 59.9	13.15	1.84	1.01	3.556	−7.21	269.2	LMC	K7 I	
146548	05 30 09.67	−69 11 03.9	13.80	2.08	1.18	3.550	−6.70	277.2	LMC	K7–M0 I	
147199	05 30 21.00	−67 20 05.7	12.73	1.57	1.20	3.484	−9.89	309.4	LMC	M4 I	M1 Ia
147257	05 30 22.20	−67 06 31.4	12.76	1.45	0.94	3.531	−8.14	302.1	LMC	M1 I	
147276	05 30 22.49	−67 05 05.9	11.94	1.33	0.71	. . .	. . .	63.3	Fgd	K2 V	
147372	05 30 24.36	−67 29 13.0	11.91	1.31	0.73	. . .	. . .	56.1	Fgd	K2 V	
147479	05 30 26.37	−69 30 24.7	12.78	1.90	1.02	3.506	−8.93	266.6	LMC	M3 I	
147928	05 30 33.55	−67 17 15.4	12.38	1.30	0.95	3.556	−7.98	291.1	LMC	K7 I	M2 I +
148035	05 30 35.61	−68 59 23.6	13.88	1.66	1.38	3.484	−8.74	284.5	LMC	M4 I	
148041	05 30 35.69	−67 12 04.3	13.06	1.81	0.99	3.531	−7.84	308.2	LMC	M1 I	
148381	05 30 41.58	−69 15 33.7	12.24	1.86	1.10	3.477	−10.71	272.6	LMC	M4.5–5	
148409	05 30 42.10	−69 05 23.2	13.32	1.81	1.05	3.538	−7.43	268.9	LMC	M0–1 I	M1 Iab
148600	05 30 45.25	−67 07 59.2	13.23	1.90	1.11	3.506	−8.48	305.2	LMC	M3 I	
149026	05 30 52.38	−67 17 34.5	12.80	1.43	0.93	3.531	−8.10	307.6	LMC	M1 I	M2 I +
149065	05 30 53.17	−67 30 52.0	12.09	1.21	0.68	. . .	. . .	−7.9	Fgd	K0 V	
149560	05 31 00.62	−69 10 39.6	13.05	0.60	1.20	3.489	−9.34	279.9	LMC	Comp I	
149587	05 31 01.19	−69 10 59.2	12.51	0.69	0.82	3.544	−8.11	278.1	LMC	M0 I	
149721	05 31 03.50	−69 05 40.0	12.71	1.86	0.97	3.562	−7.58	277.3	LMC	K5–7 I	M1 Iab
149767	05 31 04.33	−69 19 02.9	13.10	2.03	1.29	3.506	−8.61	274.4	LMC	M3 I	
150040	05 31 09.35	−67 25 55.1	12.81	1.96	1.20	3.484	−9.81	280.0	LMC	M4 I	M4 Ia−
150396	05 31 15.58	−69 03 58.8	13.26	1.81	1.15	3.525	−7.81	271.5	LMC	M1–2 I	
150577	05 31 18.56	−69 09 28.2	13.27	1.80	1.08	3.562	−7.02	277.8	LMC	K5–7 I	
150976	05 31 25.82	−69 21 17.9	13.17	1.85	1.06	3.531	−7.73	275.9	LMC	M1 I	
152132	05 31 47.50	−67 23 03.3	13.16	1.90	1.06	3.544	−7.46	292.5	LMC	M0 I	M0 Ia−
153298	05 32 08.91	−67 11 18.6	13.11	1.85	1.03	3.531	−7.79	300.9	LMC	M1 I	
153866	05 32 19.30	−67 25 00.5	13.16	1.82	1.01	3.531	−7.74	297.2	LMC	M1 I	
154311	05 32 27.54	−69 16 53.0	12.56	1.89	1.06	3.506	−9.15	261.0	LMC	M3 I	
154542	05 32 31.52	−69 20 25.7	13.02	1.94	1.01	3.544	−7.60	272.6	LMC	M0 I	
154729	05 32 35.44	−69 07 51.9	13.21	1.51	1.08	3.525	−7.86	292.0	LMC	M1–2 I	
155529	05 32 50.32	−67 27 45.3	13.34	1.84	1.20	3.506	−8.37	292.3	LMC	M3 I	
156794	05 33 14.53	−67 03 48.5	12.95	1.79	1.04	3.531	−7.95	302.7	LMC	M1 I	
157401	05 33 26.88	−67 04 13.7	12.27	1.99	1.06	3.506	−9.44	299.1	LMC	M3 I	
157533	05 33 29.67	−67 31 38.0	13.16	1.50	0.99	3.568	−7.06	302.2	LMC	K5 I	M1 Ia
158317	05 33 44.60	−67 24 16.9	13.35	1.96	1.12	3.518	−7.93	301.2	LMC	M2 I	
158646	05 33 52.26	−69 11 13.2	13.10	2.23	1.33	3.496	−8.97	288.3	LMC	M3–4 I	
159893	05 34 19.57	−68 59 36.4	13.10	1.96	1.06	3.536	−7.69	289.9	LMC	. . .	
159974	05 34 21.49	−69 21 59.8	12.72	1.77	0.91	3.580	−7.38	250.7	LMC	K2–5 I	
160170	05 34 25.97	−69 21 47.7	11.03	1.53	0.82	. . .	. . .	42.3	Fgd	K2 V	
160518	05 34 33.90	−69 15 02.3	13.10	1.89	1.17	3.525	−7.97	300.7	LMC	M1–2 I	
161078	05 34 47.07	−69 29 00.1	12.91	1.61	1.02	3.544	−7.71	269.4	LMC	M0 I	

TABLE 2—*Continued*

Star	$\alpha_{J2000.0}$	$\delta_{J2000.0}$	V	$B-V$	$V-R$	log T_{eff}[b]	M_{bol}[b]	RV[c]	Member?	Spectral Type New	Spectral Type Lit.[d]
162635	05 35 24.61	−69 04 03.2	14.23	2.33	1.36	3.531	−6.67	296.9	LMC	M1 I	
163007	05 35 32.84	−69 04 18.6	13.07	1.51	1.04	3.556	−7.29	293.8	LMC	K7 I	
163466	05 35 43.86	−68 51 21.1	12.45	1.76	1.05	3.539	−8.26	284.6	LMC	...	
163814	05 35 52.01	−69 22 28.5	12.75	1.80	0.99	3.544	−7.87	267.1	LMC	M0 I	
164506	05 36 06.44	−68 56 40.8	12.87	1.44	0.97	3.566	−7.38	288.0	LMC	...	
164709	05 36 10.56	−68 54 40.5	12.02	0.40	0.67	3.667	−7.33	287.8	LMC	...	
165242	05 36 20.42	−68 56 18.9	13.97	1.95	1.28	3.477	−8.98	289.2	LMC	...	
165543	05 36 26.91	−69 23 50.7	10.98	1.62	0.81	3.620	−8.73	277.1	LMC	K0 I	
166155	05 36 40.60	−69 23 16.4	12.94	1.51	0.96	3.556	−7.42	263.5	LMC	K7 I	
168047	05 37 20.65	−69 19 38.2	12.47	1.54	0.97	3.568	−7.75	262.1	LMC	K2–7 I	
168290	05 37 26.37	−68 47 40.1	13.23	2.03	1.18	3.496	−8.87	305.3	LMC	...	
168469	05 37 30.70	−69 02 33.2	13.50	2.24	1.14	3.562	−6.79	265.8	LMC	K5–7 I	
168757	05 37 36.96	−69 29 23.5	14.08	1.77	1.34	3.506	−7.63	272.3	LMC	M3 I	
169049	05 37 43.16	−69 24 59.6	12.65	2.02	1.14	3.518	−8.63	264.5	LMC	M1–3 I	
169142	05 37 45.15	−69 20 48.2	12.11	0.91	0.91	3.496	−9.96	264.5	LMC	M3–4 I	
169754	05 37 58.77	−69 14 23.7	13.21	2.15	1.13	3.591	−6.77	275.2	LMC	K2–3 I	
170079	05 38 06.71	−69 17 29.5	14.60	2.30	1.60	3.506	−7.11	256.5	LMC	M3 I	
170452	05 38 16.10	−69 10 10.9	13.99	2.39	1.50	3.477	−8.96	289.4	LMC	M4.5–5	
170455	05 38 16.20	−69 23 31.7	12.08	1.36	0.90	...	...	−29.1	Fgd	Dwarf	
170539	05 38 18.24	−69 17 42.1	13.86	2.14	1.29	3.506	−7.85	261.1	LMC	M3 I	
173854	05 39 46.25	−69 19 28.1	13.60	2.08	1.19	3.531	−7.30	244.8	LMC	M1 I	
174324	05 40 07.72	−69 20 05.1	13.83	1.91	1.26	3.512	−7.66	255.3	LMC	M2–3 I	
174543	05 40 17.13	−69 27 53.7	12.97	1.58	1.06	3.506	−8.74	246.9	LMC	M3 I	
174714	05 40 24.48	−69 21 16.6	13.13	1.98	1.21	3.477	−9.82	251.0	LMC	M4–5 I	
174742	05 40 25.38	−69 15 30.2	12.50	1.63	0.92	3.550	−8.00	251.4	LMC	K7–M0 I	
175015	05 40 37.04	−69 26 20.1	13.31	1.92	1.15	3.506	−8.40	249.6	LMC	M3 I	
175188	05 40 43.80	−69 21 57.8	13.52	1.72	1.36	3.512	−7.97	260.4	LMC	M2–3 I	
175464	05 40 55.36	−69 23 25.0	12.90	2.20	1.22	3.512	−8.59	245.6	LMC	M2–3 I	
175549	05 40 59.25	−69 18 36.2	13.24	2.23	1.39	3.512	−8.25	243.9	LMC	M2–3 I	M2 I
175709	05 41 05.17	−69 04 42.5	12.74	1.95	1.06	3.544	−7.88	251.7	LMC	M0 I	
175746	05 41 06.94	−69 17 14.8	13.30	2.06	1.26	3.506	−8.41	262.2	LMC	M3 I	M1 Ia−
176135	05 41 21.89	−69 31 48.8	13.06	2.10	1.26	3.506	−8.65	255.2	LMC	M3 I	
176216	05 41 24.60	−69 18 12.8	13.66	1.67	1.22	3.556	−6.70	257.5	LMC	K7 I	M1 Ia−
176335	05 41 29.70	−69 27 16.2	12.90	2.01	1.03	3.556	−7.46	247.4	LMC	K7 I	
176695	05 41 43.49	−69 28 15.4	12.92	1.97	1.03	3.544	−7.70	248.9	LMC	M0 I	
176715	05 41 44.05	−69 12 02.7	13.05	1.13	0.98	3.544	−7.57	243.7	LMC	M0 I	M1 I
176890	05 41 50.26	−69 21 15.7	12.85	1.97	1.01	3.556	−7.51	254.8	LMC	K7 I	M0 Iab
177150	05 42 00.84	−69 11 37.0	13.80	1.89	1.20	3.531	−7.10	249.0	LMC	M1 I	M1 Iab
178066	05 42 38.71	−69 09 51.4	13.30	2.00	1.05	3.556	−7.06	245.2	LMC	K7 I	M2 Ia
178555	05 43 02.16	−69 05 49.6	13.04	1.97	1.09	3.544	−7.58	269.6	LMC	M0 I	

[a] Star identifications, coordinates, and photometry are from Massey 2002.
[b] Based on spectral type, if available, or $V-R$ if not. See text.
[c] Radial velocity in units of kilometers per second.
[d] Literature spectral types are from Humphreys 1979.

with intermediate velocities. We have assigned membership in the tables based on whether or not the radial velocity is greater than 100 km s^{-1}.

Based on the radial velocities, we conclude that 11.0% of the stars in the SMC sample proved to be foreground stars, while only 5.3% of the stars in the LMC sample were foreground stars.

3.2. *Spectral Classification*

We include our spectral types in Tables 1 and 2. Not all stars were observed in the blue, and hence there are stars for which there are no spectral types. These were determined by comparison of our spectra of spectral standards with the program objects. At our dispersion and signal-to-noise ratio, the presence of TiO λ5167 suggests that the star is K5 or later, and the classification was based on the strength of the TiO bands at $\lambda\lambda$4761, 4954, 5167, 5448, and 5847. If there was no TiO present, then the relative strength of Ca I λ4226 and the G band were used to determined the spectral subtype in the range K0–K5. Strong Hγ suggested an earlier type (G-type), which proved to be the case for a few of the foreground dwarfs. The luminosity criteria are quite subtle, and we relied on our radial velocities to guide us in assigning "V" for foreground dwarfs, or "I" for supergiants. The presence of LMC giants in our sample is precluded by our V-magnitude selection criterion.

The comparison with the published spectral types for some stars in common with Elias, Frogel, & Humphreys (1985) (SMC), and Humphreys (1979) (LMC) shows generally excellent agreement. The average difference is less than half a spectral type for the 76 stars in common. In only three cases the difference is three spectral subclasses or more; i.e., SMC 026778, which we call K2 I but Elias et al. (1985) call

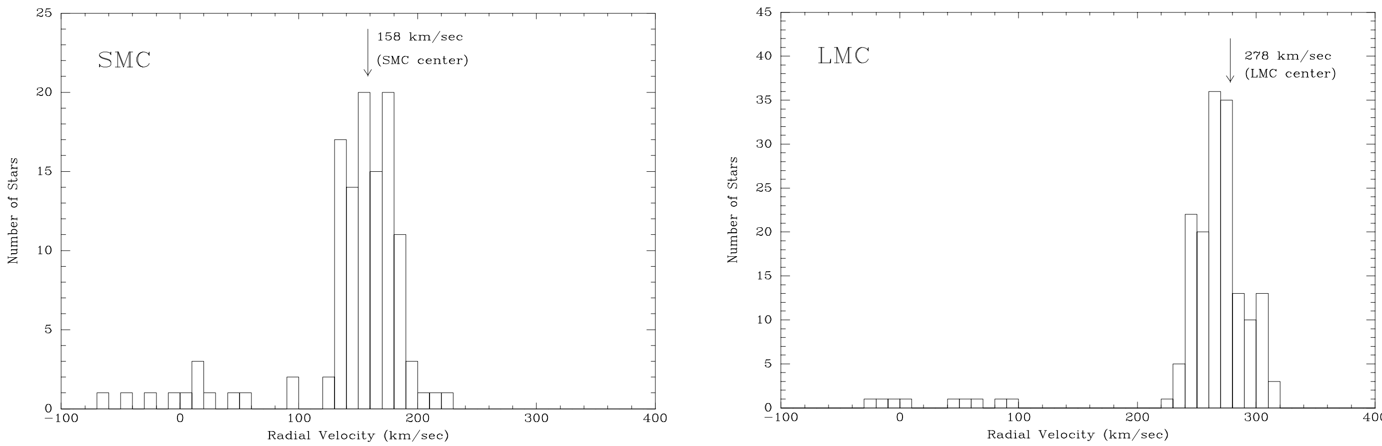

FIG. 1.—Histograms of the radial velocities are shown for the SMC and the LMC. The majority of stars have a distribution that is similar to the radial velocities of the centers of the each galaxy. The group of lower velocity (<100 km s^{-1}) stars are readily identifiable as foreground red dwarfs.

M0 I; SMC 054708, which we call K0 I but Elias et al. (1985) call M0 Iab; and LMC 178066, which we call K7 I but Humphreys (1979) call M2 Ia. Given the size of the discrepancy, we speculate that these may be spectrum variables. (In the case of the LMC star the identification is not certain, as only approximate coordinates had ever been published for the Case stars that were subsequently observed by Humphreys 1979.)

4. PHYSICAL PARAMETERS AND STELLAR EVOLUTION

What do these spectral types mean in terms of physical parameters? We have classified the stars in the traditional way, relying on the strengths of the TiO bands to determine the spectral type, with stronger bands leading to a later type. However, the metallicity (as judged from the oxygen abundances of H II regions) of the LMC is about a factor of 2 lower than in the solar neighborhood, while the metallicity of the SMC is about a factor of 4 times lower (Russell & Dopita 1990). Thus RSGs of the *same* effective temperatures in the Milky Way, LMC, and SMC would be classified as progressively earlier in these three galaxies, as lower metal abundance weakens the TiO band strength used to classify these stars. Elias et al. (1985) see such an effect in their comparison of the average (median) spectral types of RSGs in SMC (M0 I), the LMC (M1 I), and the Milky Way (M2–3 I), but they attribute the change primarily to the effect that metallicity has on the location of the (giant branch) Hayashi track, only secondarily to the effects on the spectral appearance of stars of a given effective temperature. However, modern evolutionary models do not show a Hayashi track for red *super*giants, and so it is worth reexamining this issue.

In Figure 2 we show our own histograms for the LMC and SMC supergiants in our sample and compare these with the distribution of spectral types for the Milky Way taken from Table 20 in Elias et al. (1985). The medians we find are K5–7 I for the SMC, M1 I for the LMC, and M2 I for the Milky Way. The median spectral type in the SMC is somewhat earlier than that found by Elias et al. (1985) and probably results either from our larger sample size or our better completeness for early K-type supergiants. We find, as do Elias et al. (1985), that the distribution of spectral types is more narrow in the SMC than in the LMC or Milky Way, although we still find RSGs as late as M3 I in the SMC—just not in large numbers.

First, let us ask if it is reasonable that this progression in average spectral types is due solely to the effect that metallicity has on the relationship between spectral type and effective temperature. In Table 3 we compare various effective temperature scales for Galactic RSGs. We include here the effective temperature scale adopted by Humphreys & McElroy (1984), based on a number of sources, and the Lee (1970) calibration of effective temperature with spectral types for M-type supergiants, based primarily on a very limited amount of "fundamental" data (i.e., using stars with known radii). This work has been extended considerably in recent years by Dyck et al. (1996) and Dyck, van Belle, & Thompson (1998), who obtained new interferometric observations at 2.2 μm and combined these with similar data from the literature. They provide a scale for red *giants* but consider the supergiant data to be too sparse for a calibration. Their supergiant data clearly lies several hundred degrees cooler than the giant sequence (i.e., Fig. 3 in Dyck et al. 1996). Houdashelt et al. (2000) recently compared the temperatures expected from the new MARCS models with the Dyck et al. (1996) values and found very good agreement. We have adjusted the Dyck et al. (1996) scale for red *giants* by -400 K (i.e., to cooler temperatures) to produce reasonable estimates for *supergiants*, consistent with the temperature differences illustrated in their Figure 3. (See also the discussion following Bessell 1998.) Comparing all of these values have led to a somewhat arbitrary effective temperature scale, which we adopt here, noting that the present uncertainties prevent a more definitive answer at this time. What sort of change is expected on the basis of metallicity? Improved stellar atmospheres applicable to RSGs are under construction (Gustafsson et al. 2003; Plez 2003), but until these are generally available we turn to the Atlas 9 model atmospheres of Kurucz (1992) to help answer this question.[4] Although

[4] We note that these Kurucz (1992) models are the primary component of the compilation of "standard" synthetic spectra available on the Web by T. Lejeune and collaborators, particularly in the realm of RSGs; see Fig. 1 of Lejeune, Cusinier, & Buser (1998). Although Bessell et al. (1989, 1991) have published a few models appropriate to RSGs at Galactic and SMC-like metallicities, they lack LMC-like metallicities and the grid points are sparse, causing us to adopt the Kurucz (1992) models, despite their less exact treatment of molecules.

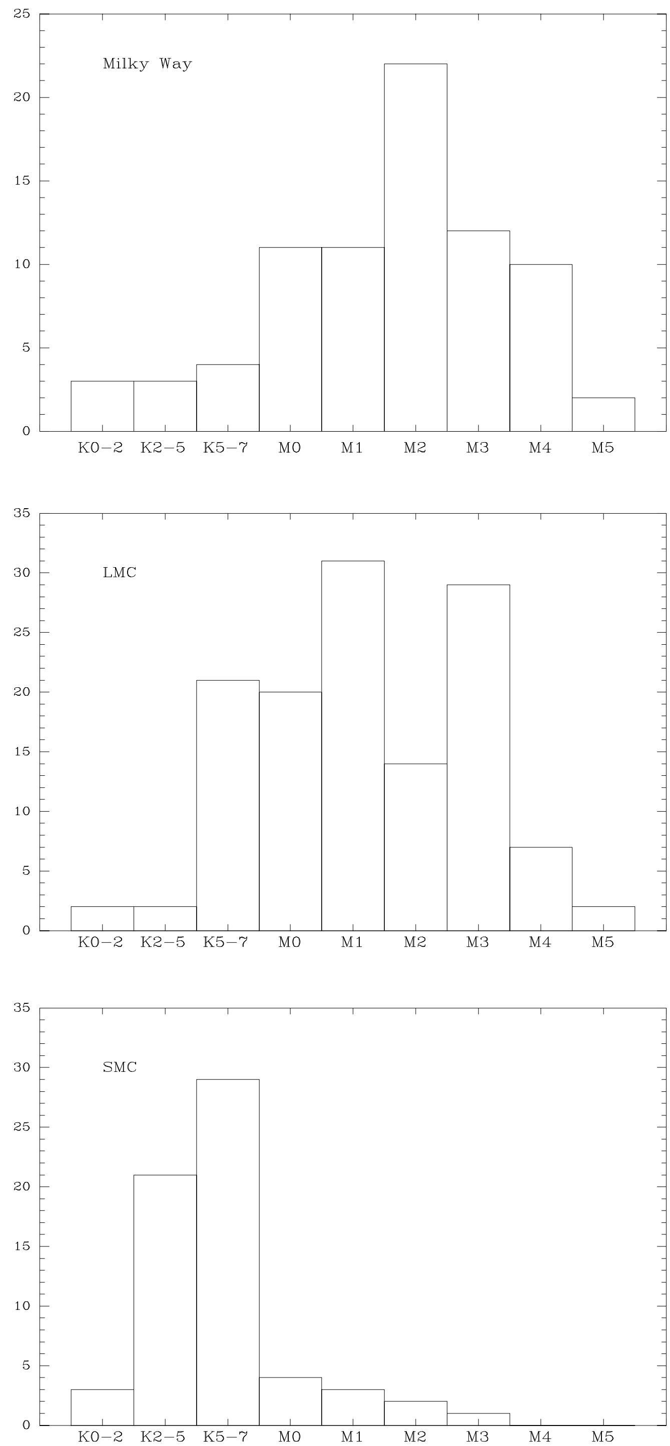

Fig. 2.—Histograms of the spectral types found in the Milky Way (Elias et al. 1985, Table 20) and the LMC and SMC (from our Tables 1 and 2, respectively). There is a progression toward earlier types. In the Milky Way the average spectral type is M2 I, in the LMC it is M1 I, and in the SMC it is K5 I.

Oestreicher & Schmidt-Kaler (1998) find that the Atlas 9 models significantly underestimate the amount of molecular absorption for *some* lines in late-type stars, we show in Figure 3 that there is pretty good agreement by comparing the coolest of Kurucz (1992) models to the spectra of three of our spectral standards. The Kurucz (1992) models correspond to solar metallicity and $\log g = 0.0$, which is appropriate for a massive supergiant.[5] We see that the 3500 K model shows TiO lines that are roughly comparable with what is seen in M0–M2 I supergiants, consistent with the effective temperature scale we adopted in Table 3. Similarly, the TiO bands in the 4000 K model are similar to that of the K2.5 I standard, also in accord with the effective temperature scale adopted above. The spectra are plotted in log units in order to facilitate comparison of band depths without the subjective task of normalization. The continuum fluxes of the stellar spectra have been adjusted by comparison with stars of similar spectral types from the Jacoby, Hunter, & Christian (1984) atlas, and so the relative fluxes are only approximate; what matters is the line depths.

We next investigate the effect the Kurucz (1992) models predict for a change in metallicity from Galactic to that of the SMC, where we have observed the spectral types change from M2 I to K5 I. The red curve in Figure 3 shows the Kurucz (1992) model for a 3500 K supergiant computed with an abundance $\log Z/Z_0 = -0.5$, while the blue curve corresponds to $\log Z/Z_0 = -1.0$. The metallicity of SMC should be intermediate between these two values. We see that metallicity alone has changed the line depths to be intermediate between the 3750 and 4000 K models. Thus, the change in metallicity from the Milky Way to that of the SMC is likely to weaken the appearance of the TiO spectral lines by an amount corresponding to +250 to +500 K. This is consistent with the $\sim$+300 K temperature difference between (Galactic) M2 I and K5–7 I stars. Thus, the effective temperature scale at lower metallicity will be cooler; i.e., an SMC M0 I star would be 300 K cooler than a Galactic M0 I star. A more quantitative comparison requires higher resolution synthetic spectra and a finer temperature and metallicity grid, and these will soon be available for such tests from the MARCS group (Gustafsson et al. 2003 and Plez 2003).[6] In the meanwhile, we will adopt an effective temperature scale for the Magellanic Cloud RSGs that is 300 K cooler for the SMC and 100 K cooler for the LMC, compared with the Milky Way, consistent with the average change in spectral type we observe.

We can provide an additional check on this by examining the intrinsic colors. It is generally recognized that $(V-R)_0$ is a good effective temperature indicator for cool stars, while $(B-V)_0$ is sensitive both to effective temperature and to surface gravity (e.g., Lee 1970; Massey 1998b; Oestreicher & Schmidt-Kaler 1999). In Table 4 we give the expected $(B-V)_0$ and $(V-R)_0$ colors as a function of effective temperature and metallicity computed from the Kurucz (1992) Atlas 9 models, where we have adopted the description of

[5] We expect that $\log g$ will vary from about -0.3 (20 $M_\odot$, $M_{\rm bol} = -8.0$, $\log T_{\rm eff} = 3.50$) to -0.6 (40 $M_\odot$, $M_{\rm bol} = -9.5$, $\log T_{\rm eff} = 3.55$). Thus the $\log g = 0.0$ Kurucz (1992) models are the most appropriate ones available for RSGs. Fortunately, the strengths of the TiO bands in general are not sensitive to the exact choice of $\log g$; see Schiavon & Barbuy (1999).

[6] B. Plez (2003, private communication) kindly gave us a chance to examine some of his models. Unfortunately, the surface gravities were $\sim$10 times that expected for a supergiant, so the application to the stars we discuss here is not straightforward. We will note that his spectra apply a considerably warmer temperature scale (and considerably more compressed) than what we adopt here. At first blush, the warmer scale appears to be in disagreement with the fundamental data of Lee (1970) and Dyck et al. (1996). The models do not show much of an effect with metallicity, but a more careful comparison done with absolute spectrophotometry, with more appropriate surface gravities, is needed.

TABLE 3

Effective Temperatures

Spectral Type	Effective Temperatures (K) HM[a]	Lee[b]	Dyck[c]	Adopted	Bolometric Corr. (mag)[d]
K2 I	4300	...	3970	4000	−0.97
K5 I	4000	...	3520	3800	−1.20
K7 I	3750	...	3490[e]	3700	−1.36
M0 I	3550	3600	3460[e]	3600	−1.50
M1 I	3450	3550	3435	3500	−1.71
M2 I	3350	3450	3340	3400	−2.00
M3 I	3250	3200	3275	3300	−2.37
M4 I	3000	2950	3195	3150	−3.09
M5 I	2800	2800	3070	3000	−4.04

[a] From Humphreys & McElroy 1984, Table 2.
[b] From Lee 1970, Table 3.
[c] From the Dyck et al. 1996 effective temperature scale for red *giants*, corrected by −400 K.
[d] From the Slesnick et al. 2002 relation between bolometric correction and effective temperature.
[e] Interpolated from spectral types K5 and M1.

the B and V bandpasses from Buser & Kurucz (1992), and that of the Kron-Cousins R passband from Bessell (1983). We include in Table 4 the approximate corresponding spectral types for Galactic stars, using Table 3. We see that there is very little change in color with metallicity for the "warmer" models (3750 to 4000 K). For the 3500 K model there is no change from the Milky Way to the LMC, but we expect that $(V-R)_0$ will be significantly larger (0.07 mag) in the SMC.

How do these colors compare with the observed photometry? In Table 5 we give the average $(B-V)_0$ and $(V-R)_0$ colors for our spectral types, where we have corrected the observed colors in Tables 1 and 2 by the average reddenings, as indicated in the footnote to the table. We have used the arithmetic means at each spectral type, after rejecting the highest and lowest values in producing these averages. We do not list colors for any spectral types with three or fewer representatives.

For the LMC there is relatively good agreement: we expect an LMC M0 I star to have $T_{\rm eff} = 3500$ K (i.e., 100 K cooler than the value listed in Table 3) and the Kurucz (1992) model atmospheres predict a $(V-R)_0$ color of 0.92. We observe 0.94 ± 0.01 (Table 5). However, for the SMC the agreement is poor between the Kurucz (1992) $(V-R)_0$ colors and those observed. If we correct the Galactic scale by −300 K as argued above, a 3500 K SMC star should have a spectral type of K5 I. The models then predict a $(V-R)_0$ color of 0.99. But what we actually observe is a $(V-R)_0$ color of 0.84. If we had made *no* correction to the Galactic effective temperature scale, then the broadband colors would be in pretty good agreement. Have we fooled ourselves in making this correction? Possibly. However, Bessell et al. (1989) has published a few models applicable to cool supergiants. We give their $(V-R)_0$ colors in Table 6. Their SMC-like metallicity ($Z = -0.5$) supergiant model predict a $(V-R)_0$ color of 0.84 at 3500 K ($\log g = -0.26$), in excellent agreement with the observed colors if we apply our temperature correction. Similarly, their $T_{\rm eff} = 3350$ K model predicts a $(V-R)_0$ color of 0.92. Applying our correction, we would expect this temperature to correspond to an SMC star of spectral type K7–M0 I, and indeed we find an observed color of 0.88–0.94, in good agreement. LMC-like metallicity models were not computed by Bessell et al. (1989), limiting the degree we can make this comparison, but we note that their Galactic $(V-R)_0$ colors are significantly bluer than the Kurucz (1992) models would predict (e.g., 0.74 vs. 0.92 at $T_{\rm eff} = 3350$ K). A finer grid of higher resolution synthetic spectra appropriate to cool supergiants is needed before a metallicity-dependent effective temperature scale can be reliably derived.

Let us next compare the distribution of stars in the H-R diagram with that predicted by stellar evolutionary models.

TABLE 4

Intrinsic Colors Computed from Kurucz (1992) Model Atmospheres

$T_{\rm eff}$ (K)	Type[d]	Galactic[a] $(B-V)_0$	Galactic[a] $(V-R)_0$[e]	LMC[b] $(B-V)_0$	LMC[b] $(V-R)_0$[e]	SMC[c] $(B-V)_0$	SMC[c] $(V-R)_0$[e]
3500	M1 I	1.79	0.92	1.82	0.92	1.84	0.99
3750	K5–7 I	1.72	0.90	1.71	0.92	1.70	0.91
4000	K2 I	1.59	0.81	1.56	0.80	1.54	0.80

[a] Computed from the Kurucz 1992 Atlas9 models with $\log g = 0.0$ and metallicity $\log Z/Z_\odot = 0.0$.
[b] Computed from the Kurucz 1992 Atlas9 models with $\log g = 0.0$ and metallicity $\log Z/Z_\odot = -0.3$.
[c] Computed from the Kurucz 1992 Atlas9 models with $\log g = 0.0$ and metallicity $\log Z/Z_\odot = -0.5$.
[d] From Table 3 for Galactic stars.
[e] $(V-R)_0$ is on the Cousins system, as described by Bessel 1983.

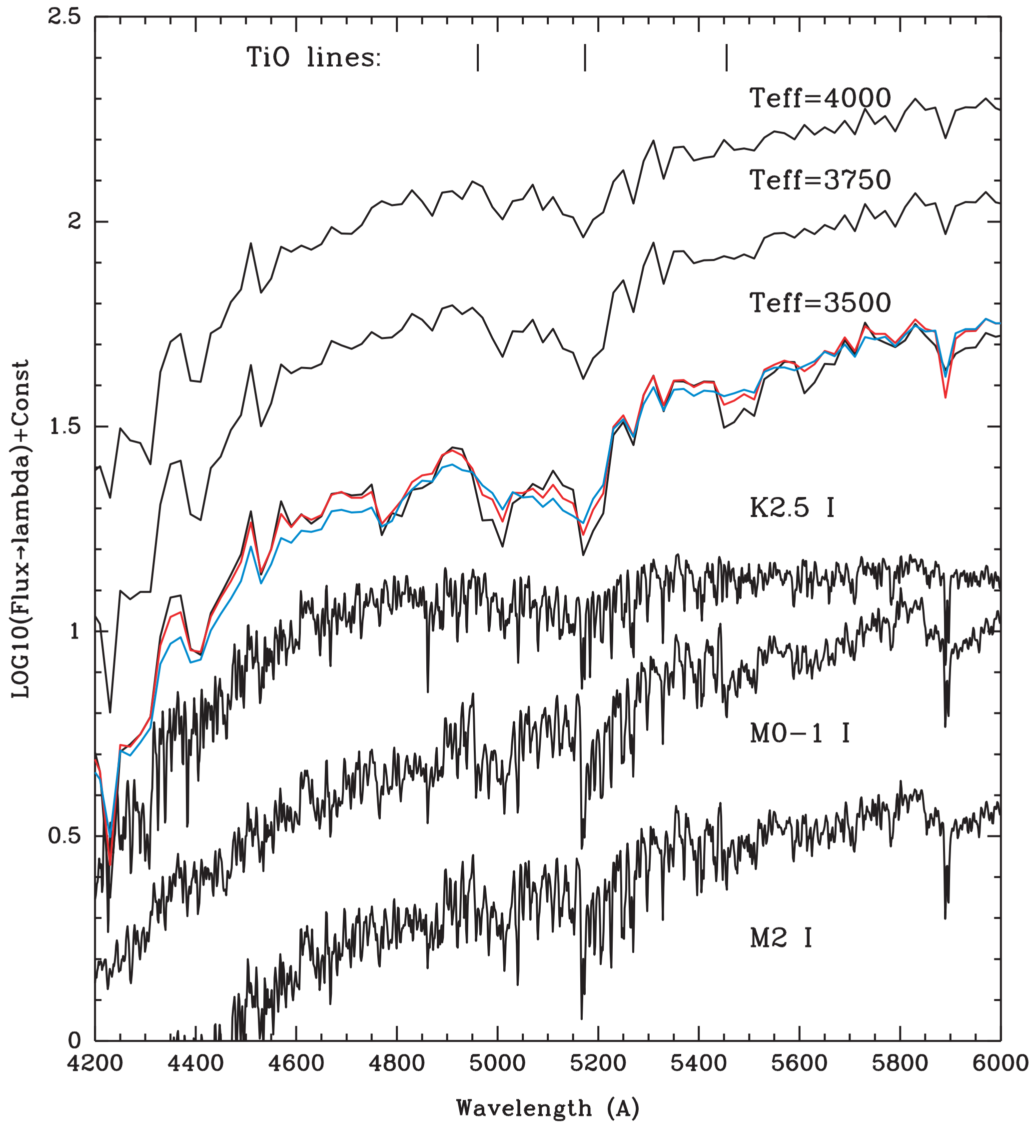

FIG. 3.—*Top three black curves*: Kurucz (1992) Atlas 9 models corresponding to Galactic metallicity ($\log Z/Z_\odot = 0.0$) and low surface gravity [$\log g(\mathrm{cgs}) = 0.0$] for $T_{\mathrm{eff}} = 4000$, 3750, and 3500 K. The spectra below demonstrate that the TiO band strengths predicted by the Galactic-metallicity 3500 K are quite similar to what are observed in M1 I stars, while the 4000 K model has lines comparable to that observed in the K2.5 I standard. The red and blue curves are 3500 K model computed with low metallicities (*red*: $\log Z/Z_\odot = -0.5$, *blue*: $\log Z/Z_\odot = -1.0$), which are included to show the effects of low metallicity on the strengths of the TiO bands. The band strengths in the low-metallicity models are intermediate between that of the higher metallicity 3750 K (K5–7 I) and 4000 K (K2 I) models, suggesting that the effect that metallicity has on the appearance on TiO lines is comparable to that observed in the distribution of spectral types seen in the SMC, LMC, and the Milky Way.

TABLE 5

MEASURED INTRINSIC COLORS

	LMC			SMC		
SPECTRAL TYPE	$(B-V)_0$[a]	$(V-R)_0$[b]	N	$(B-V)_0$[c]	$(V-R)_0$[d]	N
K2 I	...	...	...	1.57 ± 0.06	0.83 ± 0.04	7
K5 I	...	...	...	1.60 ± 0.02	0.84 ± 0.01	12
K7 I	1.63 ± 0.07	0.92 ± 0.01	11	1.65 ± 0.04	0.88 ± 0.03	23
M0 I	1.61 ± 0.08	0.94 ± 0.01	14	1.78 ± 0.02	0.94 ± 0.01	4
M1 I	1.66 ± 0.04	0.98 ± 0.02	20	...	...	
M2 I	1.76 ± 0.02	1.03 ± 0.04	5	...	...	
M3 I	1.75 ± 0.03	1.09 ± 0.02	23	...	...	
M4 I	1.55 ± 0.10	1.16 ± 0.04	5	...	...	

[a] Corrected by $E(B-V) = 0.13$.
[b] Corrected by $E(V-R) = 0.53 \times E(B-V) = 0.07$, following Savage & Mathis 1979.
[c] Corrected by $E(B-V) = 0.06$.
[d] Corrected by $E(V-R) = 0.53 \times E(B-V) = 0.03$, following Savage & Mathis 1979.

TABLE 6

Intrinsic Colors From Bessell et al. (1989) Model Atmospheres

$T_{\rm eff}$ (K)	Type[c]	Galactic[a] $(V-R)_0$[d]	SMC[b] $(V-R)_0$[d]
3000	M5 I	1.95	1.69
3200	M3–4 I	1.28	1.15
3350	M2–3 I	0.86	0.92
3500	M1 I	0.74	0.84
3650	K7–M0 I	0.69	0.79
3800	K5 I	0.65	0.73

[a] From the Bessell et al. 1989 15 $M_\odot$ models with $\log Z/Z_\odot = 0$ and $\log g$ varying from -0.11 ($T_{\rm eff} = 3800$ K) to -0.52 ($T_{\rm eff} = 3000$ K).

[b] From the Bessell et al. 1989 15 $M_\odot$ models with $\log Z/Z_\odot = -0.5$ and $\log g$ varying from -0.11 ($T_{\rm eff} = 3800$ K) to -0.52 ($T_{\rm eff} = 3000$ K).

[c] From Table 3 for Galactic stars.

[d] $(V-R)_0$ is on the Cousins system, as described by Bessel 1983.

We use the " corrected " temperatures for the spectral types, as defined above. For stars without spectral types, we can use the $(V-R)_0$ to determine an effective temperature. Comparison of our measured colors for the stars with spectral types produces two linear relations:

$$\log T_{\rm eff} = 3.899 - 0.4085 \times (V-R)_0 ({\rm SMC}),$$

$$\log T_{\rm eff} = 3.869 - 0.3360 \times (V-R)_0 ({\rm LMC}).$$

The conversion from the adopted effective temperatures to bolometric corrections is made by using the relation of Slesnick, Hillenbrand, & Massey (2002), which is primarily a fit to the bolometric corrections as a function of effective temperatures tabulated by Humphreys & McElroy (1984). We have included the adopted $T_{\rm eff}$ and $M_{\rm bol}$ in Tables 1 and 2.

As the Massey (2002) photometric survey was limited in area and could conceivably suffer from saturation for the most luminous supergiants, we should also consider other stars that have been spectroscopically confirmed as Magellanic Cloud RSGs. We list these in Tables 7 and 8. In the case of the SMC we have excellent cross-reference to the spectral types of Elias et al. (1985), thanks to the good coordinates provided by Sanduleak (1989). However, cross-referencing to the spectral types of Humphreys (1979) was more of a challenge, as only approximate coordinates were provided in the Case objective prism survey (Sanduleak & Philip 1977) from which Humphreys (1979) drew her sample for spectroscopy. Thus, Massey (2002) gives all cross-identifications for the LMC stars as tentative, and there

TABLE 7

Other Spectroscopically Confirmed RSGs in the SMC

ID	V	Other ID[a]	Spectral Type[b]	$\log T_{\rm eff}$	$M_{\rm bol}$
From Massey 2002					
003196	13.11	SkKM13	M1 I	3.505	−8.75
018136	11.98	SkKM63	M0 Ia	3.518	−9.43
021362	12.89	SkKM78	K5–M0 I	3.531	−8.15
021381	12.81	SkKM79	K5–M0 I	3.531	−8.23
023401	12.99	SkKM89	K5 I	3.544	−7.75
035445	12.74	SkKM144	M0 Iab	3.518	−8.67
069886	11.74	SkKM319	M2 Ia	3.491	−10.70
From Elias et al. 1985					
101-6	12.67	SkKM13	M1 I	3.505	−9.19
106-1a	12.24	SkKM63	M0 Ia	3.518	−9.17
105-7	12.80	SkKM78	K5–M0 I	3.531	−8.24
106-5	12.95	SkKM79	K5–M0 I	3.531	−8.09
106-7	13.12	SkKM89	K5 I	3.544	−7.62
106-9	13.16	SkKM91	K5–M0 I	3.531	−7.88
108-3	12.56	SkKM110	M0 I	3.518	−8.85
105-11	12.38	SkKM114	M0 Iab	3.518	−9.03
108-8	13.19	SkKM129	K0–2 I	3.568	−7.17
105-21	13.68	SkKM135	K5–M0 I	3.531	−7.36
HV 838	13.35	SkKM142	M0e I	3.518	−8.06
114-3	12.89	SkKM144	M0 Iab	3.518	−8.52
HV 11423	11.77	SkKM205	M0 Ia	3.518	−9.64
115-6	12.92	SkKM210	K1–3 Iab	3.568	−7.44
116-15	12.05	SkKM236	M0 Ia	3.518	−9.36
115-17	13.03	SkKM237	K5–M0 Iab	3.531	−8.01
120-14	11.96	SkKM275	K5–M0 Iab	3.531	−9.08
HV 2084	12.62	SkKM319	M2 Ia	3.491	−9.82
HV 2228	12.89	SkKM347	M0 Iab	3.518	−8.52
108-2	12.28	. . .	M0 Ia	3.518	−9.13
118-18	13.32	SkKM272?	M0 Ia	3.518	−8.09

[a] Identification from Sanduleak 1989.

[b] Spectral types are all from Elias et al. 1985.

TABLE 8
Other Spectroscopically Confirmed RSGs in the LMC

ID	V	Other ID[a]	Spectral Type[b]	log $T_{\rm eff}$	$M_{\rm bol}$
From Massey 2002					
141430	12.30	46-32	M0 Ia	3.544	−8.32
141772	12.55	46-34	M2 Ia	3.518	−8.73
156011	12.11	53-3	M0 Ia	3.544	−8.51
From Humphreys 1979					
46-40	12.98	. . .	M1 Ia	3.531	−7.92
45-48	13.38	. . .	M4 Ia–Iab	3.484	−9.24
54-35	12.85	. . .	M1 I+B	3.531	−8.05
54-47a	13.10	. . .	M1 Iab	3.531	−7.80
45-2	12.90	. . .	M2 Iab	3.518	−8.38
37-32	12.95	. . .	M2 I	3.518	−8.33
37-35	12.89	HV916	M3 Ia	3.506	−8.82
37-24	13.59	HV2360	M2 Ia	3.518	−7.69
39-33	12.57	HV888	M4 Ia	3.484	−10.05
46-2	12.25	HV2450	M2 Ia	3.518	−9.03
61-23	13.28	. . .	M1 Ia–Iab	3.531	−7.62
53-3	12.04	. . .	M0 Ia	3.544	−8.58
46-31	13.00	HV2567	M2 Iab	3.518	−8.28
46-51	12.84	HV2602	M2 Ia–Iab	3.518	−8.44
46-52	13.40	. . .	M1 Iab	3.531	−7.50
54-47	13.02	. . .	M0 Iab	3.544	−7.60
54-39	12.76	HV2781	M1 Ia–Iab	3.531	−8.14
54-38	13.03	. . .	M2 Ia	3.518	−8.25
54-56	13.32	. . .	M0 Ia–Iab	3.544	−7.30
54-44	13.03	. . .	M1 Ia–Iab	3.531	−7.87
55-20	13.09	. . .	M2 Ia–Iab	3.518	−8.19
52-4	13.00	HV5914	M1 Iab	3.531	−7.90

[a] As given in Humphreys 1979.
[b] Spectral types are all from Humphreys 1979.

were a number of stars for which several possible matches were a possibility. Thus, there may be other previously observed LMC RSGs that we have incorrectly adopted as identical to our stars in Table 2.

We show the H-R diagrams in Figures 4 and 5, where we include the evolutionary tracks both of the Geneva and Padua groups (Schaerer et al. 1993; Meynet et al. 1994; Fagotto et al. 1994). We see here a very interesting effect, namely, that *none* of these evolutionary tracks produce RSGs that are as cool and as luminous as observed in the Magellanic Clouds. Although the agreement is good at 12 $M_\odot$, at higher masses the tracks simply do not go far enough to the right (cool temperatures) to produce the RSGs that we observe. It would appear that the RSG sequence extends up to perhaps 40 $M_\odot$, but that those tracks simply do not go sufficiently far to the right in the diagram. Massey (2003a, 2003b) finds that the identical problem exists for Galactic RSGs, even when adopting the effective temperature scale and luminosities of Humphreys (1978).

This discrepancy has also been suggested by the poor match of synthetic "starburst" spectra to observations of the integrated light of various stellar populations (e.g., Mayya 1997; Oliva & Origlia 1998; Origlia et al. 1999). It is quite apparent even if one looks only at the broadband colors derived by Lejeune & Schaerer (2001). For instance, if one considers the 40 $M_\odot$ evolutionary track computed with $Z = 0.004$ and a normal mass-loss rate by Charbonnel et al. (1993), which is shown in Figure 4*a*. Lejeune & Schaerer 2001) compute $B-V = 0.244$ and $V-R = 0.157$ at the coolest extension of the track. These colors correspond to a mid–F-type supergiant.

What can account for the problem with the evolutionary tracks? One possibility is the difference that the treatment of convection can make in the evolutionary tracks. This is illustrated in Figure 9 of Maeder & Meynet (1987), where they compare the older Böhm-Vitense (1981) mixing length (1.5 times the local pressure scale height) with a more accurate treatment that includes the effects of turbulent pressure and acoustic flux and has the mixing length proportional to the density scale height. Although the physics is better, the result is that the evolutionary tracks no longer produce RSGs that are as luminous and cool as earlier models had. However, the Padua models reply on the older Böhm-Vitense (1981) prescription, albeit it with a mixing length of 1.63 times the pressure scale height, and these too suffer from the same problem, as shown in Figures 4 and 5. Maeder & Meynet (1987) were certainly aware of the mismatch between theory and observation, and they expressed the hope that "complete stellar models" (i.e., ones that included the extended atmospheres caused by stellar winds) would some day alleviate the problem. Such winds would make the star larger than the (purely) interior models would suggest, lowering the effective temperature. In the meanwhile, this discrepancy has been generally ignored by the users of these models.

What if we had ignored the effective temperature corrections? In Figure 6 we compare the H-R diagrams for the SMC and LMC, adopting the Galactic spectral type to

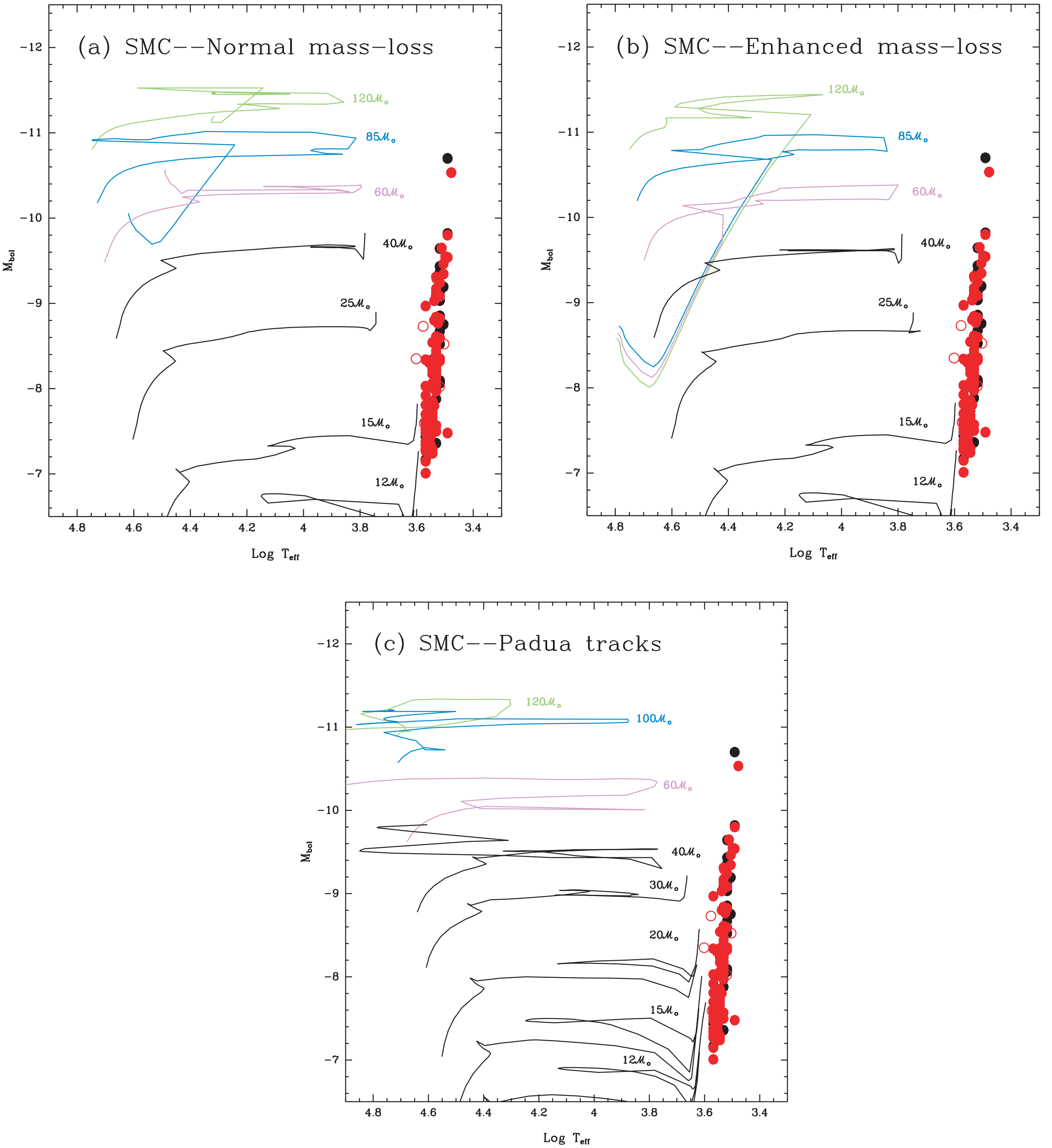

FIG. 4.—Location of the SMC RSGs in the HRD is compared with three sets of $Z = 0.004$ evolutionary tracks. (*a*) Geneva models which include normal mass-loss rates (Charbonnel et al. 1993); (*b*) Geneva models, which include "enhanced" (2 times normal) mass-loss rates (Meynet et al. 1994); and (*c*) the Padua models, which also use normal mass-loss rates (Fagotto et al. 1994). In none of these cases do the models produce RSGs that are as cool and luminous as actually observed. The solid points are been placed in the diagram using their spectral types to set the effective temperature, while the open circles have used the photometry to determine the effective temperature. Red points are data from this paper, while black points are taken from the literature (i.e., Elias et al. 1985).

effective temperature calibration from Table 3 and computing the corresponding color to effective temperature equation. It is clear that, if we had made no correction, the RSGs would be of considerably higher luminosity in the LMC than in the SMC. In the left-hand side of Figure 7 we compare the distribution of bolometric luminosities for RSGs both with and without these corrections. We see that, without the corrections, the number of RSGs in the SMC drops

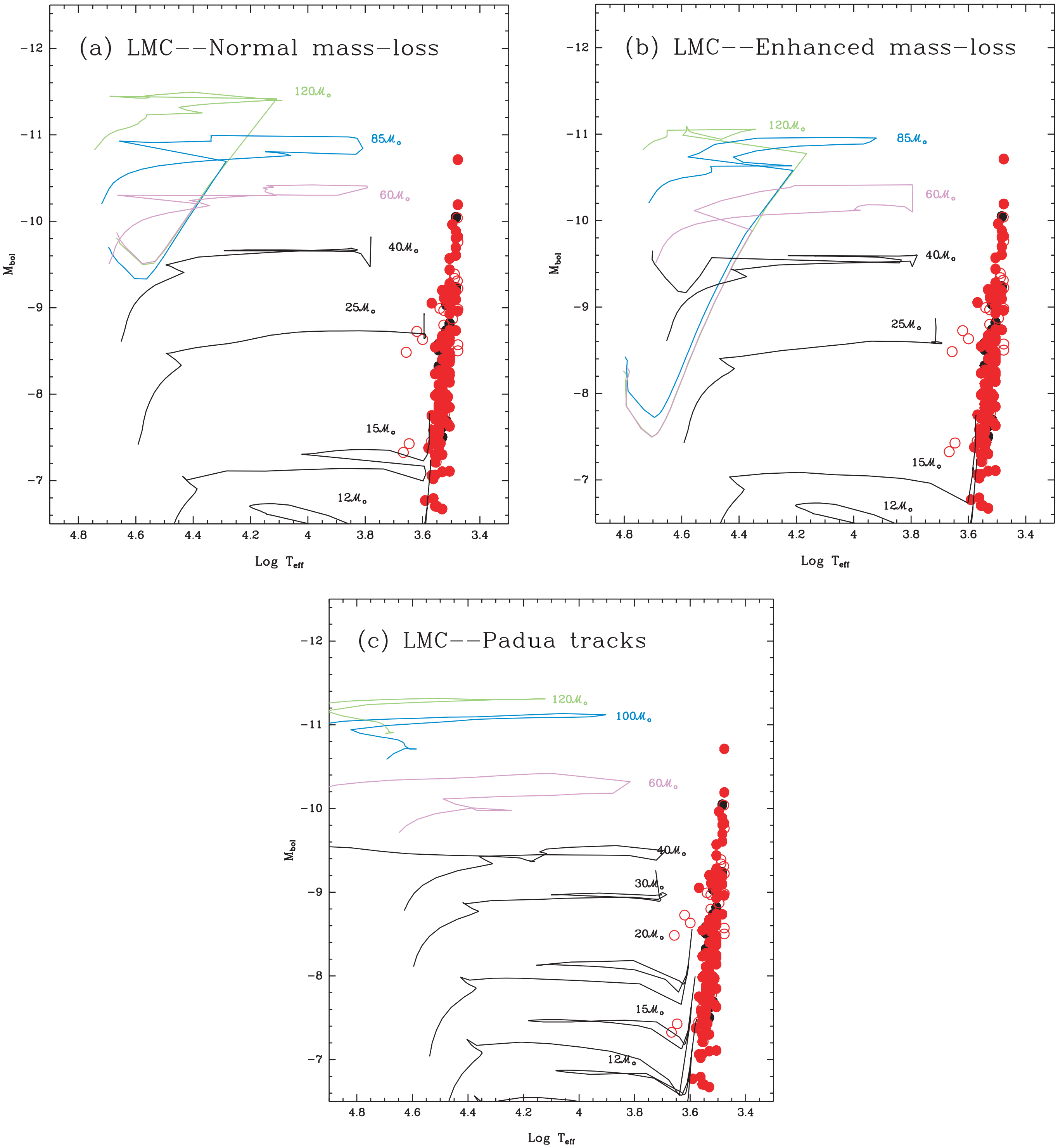

FIG. 5.—Location of the LMC RSGs in the HRD is compared with three sets of $Z = 0.008$ evolutionary tracks. (*a*) Geneva models, which include normal mass-loss rates (Schaerer et al. 1993); (*b*) Geneva models, which include "enhanced" (2 times normal) mass-loss rates (Meynet et al. 1994); and (*c*) Padua models, which also uses normal mass-loss rates (Fagotto et al. 1994). In none of these cases do the models produce RSGs that are as cool and luminous as actually observed. The solid points are been placed in the diagram using their spectral types to set the effective temperature, while the open circles have used the photometry to determine the effective temperature. The red points are data from this paper, while black points are taken from the literature (i.e., Humphreys 1979).

very abruptly with increasing luminosity compared with the LMC. This runs counter to the expected evolutionary effect that, at lower metallicities, higher mass (luminosity) stars should spend a greater fraction of their He-burning lifetimes as RSGs rather than WRs, since mass-loss rates will be lower at low metallicities (see Maeder et al. 1980 and Maeder & Conti 1994). Indeed, Massey (1998b) found a smooth decrease in the numbers of the highest luminosity

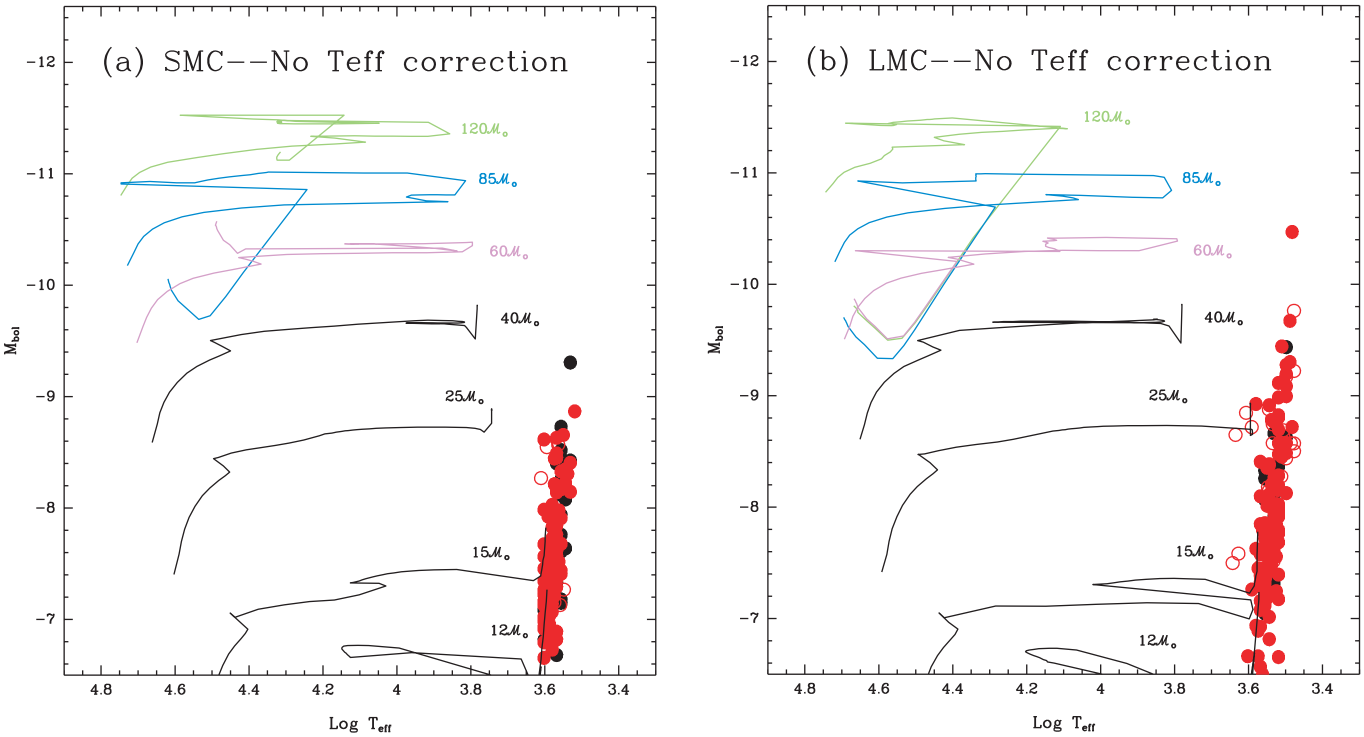

FIG. 6.—Data from Figs. 4 and 5 plotted as if we had adopted the Galactic effective temperature scale. The evolutionary tracks shown are (*a*) the Geneva normal mass-loss tracks ($Z = 0.004$) for the SMC from Charbonnel et al. (1993) and (*b*) the Geneva normal mass-loss tracks ($Z = 0.008$) for the LMC from Schaerer et al. (1993). Note that there is now a deficiency of the higher luminosity RSGs in the SMC (*a*) compared with that of the LMC (*b*). Such an effect runs counter to the expectations of stellar evolution and gives some addition credence to the corrections adopted earlier.

RSGs as metallicity increased from NGC 6822 (SMC-like) to M33 (LMC-like) to M31 (higher than solar). When we make the correction for effective temperature, however, the luminosity functions become very similar (*right-hand side*, Fig. 7). Thus, either a significant correction to the Galactic $T_{\rm eff}$ scale is needed for SMC RSGs, as we have made above, or else there is an unexpected absence of higher luminosity RSGs in the SMC.

We note that, in the case of the H-R diagrams with the corrected temperatures, we expect that the most luminous RSGs come from stars with initial masses of about 40 $M_\odot$. This is consistent with the so-called upper luminosity limit described by Humphreys & Davidson (1979) and explained by Lamers (1997): the "modified" Eddington limit should prevent stars with luminosities above $M_{\rm bol} \sim -10$ from evolving to the right in the H-R diagram. This limit should, if anything, be slightly higher at lower metallicities, since the opacities will be lower, and thus is consistent with our corrected temperatures.

Perhaps one of the most interesting things to be apparent in the H-R diagrams is that there is a very smooth decrease in effective temperature with increasing luminosity, whether or not the temperature corrections are applied. *The higher luminosity RSGs are invariably of cooler effective temperatures.* This tight sequence is obviously not reproduced by the stellar evolutionary models. Explaining this simple sequence provides an important challenge to stellar evolutionary theory.

Finally, let us briefly reconsider the ratio of blue-to-red supergiants (B/R) in the SMC and the LMC. As emphasized in Massey (2002, 2003a), one needs to be careful in what one is counting for this ratio to have much meaning. We need to include K-type as well as M-type stars, but would like to exclude stars earlier than K type, as the degree of foreground contamination increases at intermediate colors. We adopt the same convention as Massey (2002), namely, $(V-R)_0 > 0.6$, corresponding to a star of log $T_{\rm eff} = 3.66$ (4600 K, or late G type). We also restrict ourselves to counting only stars with $M_{\rm bol} < -7.5$, as less luminous than this there is a chance of contamination by intermediate-mass asymptotic giant branch stars (Brunish, Gallagher, & Truran 1986). In counting stars, we include all of the sufficiently luminous RSGs in Tables 1 and 2, plus a fraction of the other red stars from Massey (2002). Our spectroscopy suggests that 11% of the red stars seen toward the SMC, and 5.3% of the red stars seen toward the LMC, are foreground, so we count only 89% and 94.7% of the remainder.[7] We find that we expect about 90 RSGs in the SMC sample, and 234 RSGs in the LMC sample. For the blue stars, we use the numbers given in Table 10 of Massey (2002, 2003a), i.e., all of the stars in the SMC and LMC areas surveyed that meet the criteria $M_{\rm bol} < -7.5$ and $(B-V)_0 < 0.14$, where the latter roughly corresponds to the color of an A9 I star (log $T_{\rm eff} = 3.9$). We then count 1484 blue supergiants in the SMC and 3164 blue supergiants in the LMC, although these numbers are considerably uncertain given the difficulty in converting photometry to log $T_{\rm eff}$ and $M_{\rm bol}$ for hot stars. (See, e.g., Massey1998a.) The derived B/R values are thus

[7] Since we have adopted a new conversion between $(V-R)_0$ and log $T_{\rm eff}$, we started with the complete photometric catalog (Table 3) of Massey (2002) rather than the list of just the red, luminous stars (Table 9), but the differences are small.

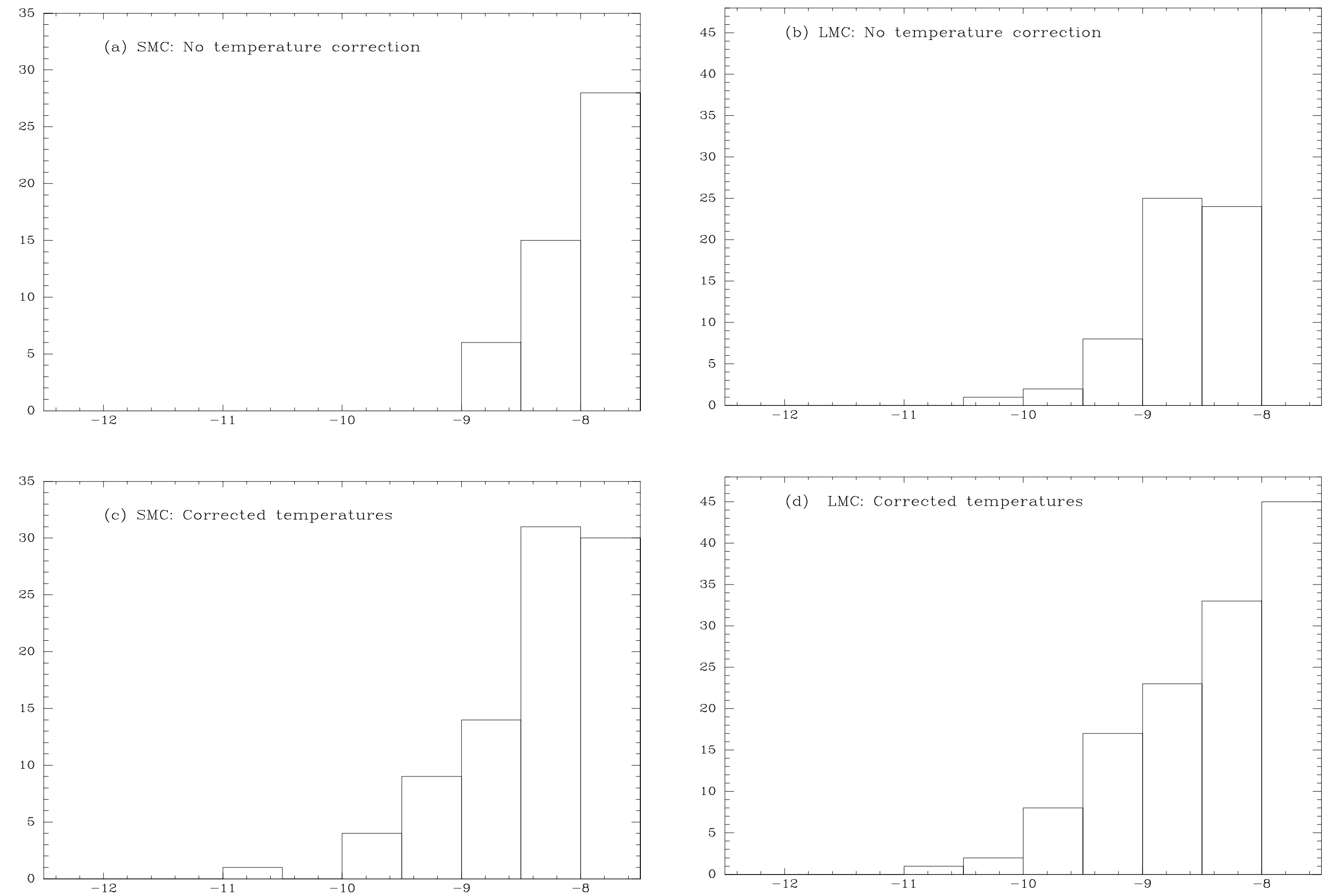

FIG. 7.—(*a*) and (*b*): Relative number of RSGs as a function of bolometric luminosity if we had made no temperature correction to the Galactic scale. The number of high-luminosity RSGs drops fars more steeply in the SMC (*a*) than in the LMC (*b*), contrary to the expectations of stellar evolution. (*c*) and (*d*): The same histograms for the " corrected " temperature scales. Here the distributions are very similar, although incompleteness may affect the lowest luminosity bin for the SMC (*c*). We have included only the confirmed RSGs from this paper.

16 for the SMC and 14 for the LMC, essentially identical. Massey (2002, 2003a) notes that a large (factor of 3) difference is found if only M-type stars are counted. Thus, the fact that the stellar models fail to reproduce the " observed " B/R value (Langer & Maeder 1995) may be in large part due to the differences in how the " observed " ratios have actually been counted. The slightly different approach here has changed the B/R ratio given by Massey (2002) by nearby a factor of 2 in itself, and thus we again emphasize the large " observational " uncertainty in such a census, as the derived ratio is highly sensitive to the conversions to bolometric luminosity.

We can compare this number with that predicted from stellar models. For this comparison we follow the advice offered by Schaerer & Vacca (1998) to determine the number of stars from the model by integrating the initial mass function over closely spaced isochrones, rather than by integrating over the coarsely spaced mass tracks. The SMC-like $Z = 0.004$ Geneva models with normal mass-loss rates (Charbonnel et al. 1993) predict a blue-to-red supergiant ratio of 54, while the enhanced mass-loss models (Meynet et al. 1994) would expect a blue-to-red supergiant ratio of 36. The LMC-like $Z = 0.008$ Geneva models with normal mass-loss rates (Schaerer et al. 1993) predict a B/R value of 10, while those using enhanced mass-loss rates (Meynet et al. 1994) predict a B/R value of 3. Thus, the lower metallicity models (SMC-like) predict a much higher ratio of B/R than what is observed, while the intermediate metallicity models (LMC-like) predict a somewhat lower value. Given that we have earlier shown that the models fail to reproduce the location of RSGs in the H-R diagram, the disagreement is not surprising. Maeder & Meynet (2001) find that more RSGs are produced in the models at SMC-like metallicities when rotation is included. Comparisons with the new rotation models that cover a range of metallicities will be of great interest.

5. SUMMARY AND CONCLUSIONS

We have examined samples of red stars seen toward the SMC and LMC. Our spectroscopy has been able to determine membership based on radial velocity information; we find that the contamination by foreground red dwarfs is about 11% in the SMC sample and 5.3% in the LMC sample.

Classification of our spectra confirms that there is a progression in the average spectral type of RSGs with metallicity. RSGs in the SMC (which is the lowest in metallicity) have an average spectral type of K5–7 I. Nevertheless, there are a few SMC RSGs as late as M3 in our sample. In the

LMC RSGs have an average type of M1 I, while those in the Milky Way have an average type of M2 I. At lower metallicity the appearance of the TiO lines (used as the primary classification criterion) should be weaker, and examination of the Kurucz (1992) Atlas 9 models suggests that this effect is probably sufficient in itself to account for the shift in average spectral types observed. If so, then RSGs in the SMC are about 300 K cooler than Galactic stars of the same spectral types, while RSGs in the LMC are about 100 K cooler. The $(V-R)_0$ colors predicted by the Kurucz (1992) models do not agree with this conclusion; but other models (e.g., Bessell 1989) show better agreement with the SMC data, although they lack the LMC-like metallicity we would need to draw conclusions. Good resolution (<10 Å) synthetic spectra for red supergiants ($\log g = 0.0$) covering a range of metallicities is needed (along with good spectrophotometry) to address this discrepancy.

We find that none of the stellar evolutionary models produce RSGs that are as red and luminous as observed in the Magellanic Clouds. This discrepancy may be due to the treatment of convection in the evolutionary models, or it could simply be due the lack of inclusion of that stellar winds have in increasing the atmosphere extent (leading to a decrease in the effective temperature) in the stellar models. Nevertheless, the location of RSGs compared with the evolutionary tracks suggests that the most luminous RSGs have evolved from stars with initial masses of 40 $M_\odot$, in accord with previous studies. We show that ignoring the temperature correction described above would lead to an underabundance of high-luminosity SMC RSGs.

There is a very tight sequence in the H-R diagram in which the higher luminosity RSGs are of lower effective temperatures. Matching this sequence will be an important test of future stellar models.

The blue-to-red supergiant ratio does not appear to be significantly different in the SMC than in the LMC, although there is still considerable uncertainty in the number of blue supergiants in our sample. This work has underscored the point made by Massey (2002), that the B/R value is very dependent on how stars are counted, and thus disagreements with the predictions of stellar evolutionary models have to be carefully evaluated. Using the non-rotation Geneva models, we find that the SMC-like ($Z = 0.004$) models predict too large a value for B/R, while the LMC-like ($Z = 0.008$) models predict too small a value. Given the fact that the models fail to produce high-luminosity red supergiants, such disagreements are not surprising. The effects that rotation will have on the predicted B/R ratio as a function of metallicity remain unclear. As Maeder & Meynet (2000) describe, the additional mixing caused by rotational instabilities would tend to produce few RSGs, while, on the other hand, higher rotation will lead to increase mass loss, and this would tend to produce more RSGs. The result is that it is still unclear what affect, if any, the complete inclusion of rotation will have on the predictions of B/R ratios as a function of metallicities, although Maeder & Meynet (2001) find that at a SMC-like metallicity including rotation will lower the predicted B/R ratio, which goes in the correct direction. Eggenberger, Meynet, & Maeder (2002) compare the observed B/R ratios of clusters with those of models, but, as discussed extensively by Massey (2002, 2003a, 2003b), the "B/R" ratio in a quasi-coeval situation will be quite different than in a mixed-age population, such as what we consider here.

This work was supported by NSF Grant AST 00-93060. We are grateful, as always, to the kind hospitality and excellent support by the technical staff at CTIO. We also benefited from correspondence with Ken Hinkle and Daniel Schaerer. Deidre Hunter offered useful comments on an early draft of this manuscript.

REFERENCES

Abbott, D. C. 1982, ApJ, 259, 282
Armandroff, T. E., & Massey, P. 1985, ApJ, 291, 685
Barden, S. C., & Ingerson, T. E. 1998, in ASP Conf. Ser. 152, Fiber Optics in Astronomy III, ed. S. Arribas, E. Mediavilla, & F. Watson (San Francisco: ASP), 60
Bessell, M. S. 1983, PASP, 95, 480
———. 1998, in IAU Symp. 189, Fundamental Stellar Properities: The Interaction between Observation and Theory, ed. T. R. Bedding, A. J. Booth, & J. Davis (Dordrecht: Kluwer), 127
Bessell, M. S., Brett, J. M., Scholz, M., & Wood, P. R. 1989, A&AS, 77, 1
———. 1991, A&AS, 89, 335
Böhm-Vitense, E. 1981, ARA&A, 19, 295
Brunish, W. M., Gallagher, J. S., &Truran, J. W. 1986, AJ, 91, 598
Brunish, W. M., & Truran, J. W. 1982, ApJ, 256, 247
Buser, R., & Kurucz, R. L. 1992, A&A, 264, 557
Charbonnel, C., Meynet, G., Maeder, A., Schaller, G., & Schaerer, D. 1993, A&AS, 101, 415
Chiosi, C., Nasi, E., & Bertelli, G. 1979, A&A, 74, 62
Chiosi, C., Nasi, E., & Sreenivasan, S. R. 1978, A&A, 63, 103
Crowther, P. A., Dessart, L., Hillier, D. J., Abbott, D. B., & Fullerton, A. W. 2002, A&A, 392, 653
de Jager, C., Nieuwenhuijzen, H., & van der Hucht, K. A. 1988, A&AS, 72, 259
de Loore, C., De Grève, J. P., & Lamers, H. J. G. L. M. 1977, A&A, 61, 251
de Loore, C., De Grève., J. P., & Vanbeveren, D. 1978, A&A, 67, 373
Dyck, H. M., Benson, J. A., van Belle, G. T., & Ridgway, S. T. 1996, AJ, 111, 1705
Dyck, H. M., van Belle, G. T., & Thompson, R. R. 1998, AJ, 116, 981
Eggenberger, P., Meynet, G., & Maeder, A. 2002, A&A, 386, 576
Elias, J. H., Frogel, J. A., & Humphreys, R. M. 1985, ApJS, 57, 91
Fagotto, F., Bressan, A., Bertelli, G., & Chiosi, C. 1994, A&AS, 105, 29
Gustafsson, B., Edvardsson, B., Eriksson, K., Mizuno-Wiedner, M., Grae-Jorgensen, U., & Plez, B. 2003, in ASP Conf. Ser. 288, Stellar Atmosphere Modeling, ed. I. Hubeny, D. Mihalas, & K. Werner (San Francisco: ASP), 331
Houdashelt, M. L., Bell, R. A., Sweigard, A. V., & Wing, R. F. 2000, AJ, 119, 1424
Humphreys, R. M. 1978, ApJS, 38, 309
———. 1979, ApJS, 39, 389
Humphreys, R. M., & Davidson, K. 1979, ApJ, 232, 409
———. 1994, PASP, 106, 1025
Humphreys, R. M., & McElroy, D. B. 1984, ApJ, 284, 565
Jacoby, G. H., Hunter, D. A., & Christian, C. A. 1984, ApJS, 56, 257
Kudritzki, R. P. 2002, ApJ, 2002, ApJ, 577, 389
Kudritzki, R. P., Pauldrach, A., Puls, J., & Abbott, D. C. 1989, A&A, 219, 205
Kudritzki, R. P., & Puls, J. 2000, ARA&A, 38, 613
Kurucz, R. L. 1992, in IAU Symp. 149, The Stellar Populations of Galaxies, ed. B. Barbuy & A. Renzini (Dordrecht: Kluwer), 225
Lamers, H. J. G. L. M. 1997, in ASP Conf. Ser. 120, Luminous Blue Variables: Massive Stars in Transition, ed. A. Nota & H. J. G. L. M. Lamers (San Francisco: ASP), 76
Lamers, H. J. G. L. M., & Cassinelli, J. P. 1996, in ASP Conf. Ser. 98, From Stars to Galaxies: The Impact of Stellar Physics on Galaxy Evolution, ed. C. Leitherer, U. Fritze-von Alvensleben, & J. Huchra (San Francisco: ASP), 162
Langer, N., & Maeder, A. 1995, A&A, 295, 685
Lee, T. A. 1970, ApJ, 162, 217
Lejeune, T., Cuisinier, F., & Buser, R. 1998, A&AS, 130, 65
Lejeune, T., & Schaerer, D. 2001, A&A, 366, 538
Maeder, A., & Conti, P. S. 1994, ARA&A, 32, 227
Maeder, A., Lequeux, J., & Azzopardi, M. 1980, A&A, 90, L17
Maeder, A., & Meynet, G. 1987, A&A, 182, 243
———. 2000, ARA&A, 38, 143
———. 2001, A&A, 373, 555
———. 2002, in IAU Symp. 212, A Massive Star Odyssey, From Main Sequence to Supernova, ed. K. A. van der Hucht, A. Herrero, & C. Esteban (San Francisco: ASP), 267
Massey, P. 1998a, in ASP Conf. Ser. 142, The Stellar Initial Mass Function, ed. G. Gilmore & D. Howell (San Francisco: ASP), 17

Massey, P. 1998b, ApJ, 501, 153
———. 2002, ApJS, 141, 81
———. 2003a, in IAU Symp. 212, A Massive Star Odyssey, From Main Sequence to Supernova, ed. K. A. van der Hucht, A. Herrero, & C. Esteban (San Francisco: ASP), 316
———. 2003b, ARA&A, 41, 15
Massey, P., & Johnson, O. 1998, ApJ, 505, 793
Massey, P., Lang, C. C., DeGioia-Eastwood, K., & Garmany, C. D. 1995, ApJ, 438, 188
Mayya, Y. D. 1997, ApJ, 482, L149
Meynet, G., & Maeder, A. 2002, A&A, 390, 561
Meynet, G., Maeder, A., Schaller, G., Schaerer, D., & Charbonnel, C. 1994, A&AS, 103, 97
Morgan, W. W., & Keenan, P. C. 1973, ARA&A, 11, 29
Oestreicher, M. O., & Schmidt-Kaler, T. 1998, MNRAS, 299, 625
———. 1999, Astron. Nachr. 320, 385
Oliva, E., & Origlia, L. 1998, A&A, 332, 46
Origlia, L., Goldader, J. D., Leitherer, C., Schaerer, D., & Oliva, E. 1999, ApJ, 514, 96
Pauldrach, A., Puls, J., & Kudritzki, R. P. 1986, A&A, 164, 86
Plez, B. 2003, in GAIA Spectroscopy, Science, and Technology, ed. U. Munari (San Francisco: ASP), 189
Puls, J., et al. 1996, A&A, 305, 171
Puls, J., Springmann, U., & Lennon, M. 2000, A&AS, 141, 23
Russell, S. C., & Dopita, M. A. 1990, ApJS, 74, 93
Salasnich, B., Bressan, A., & Chiosi, C. 1999, A&A, 342, 131
Sanduleak, N. 1989, AJ, 98, 825
Sanduleak, N., & Philip, A. G. D. 1977, Publ. Warner and Swasey Obs., 2, 105
Savage, B. D., & Mathis, J. S. 1979, ARA&A, 17, 73
Schaerer, D., Meynet, G., Maeder, A., & Schaller, G. 1993, A&AS, 98, 523
Schaerer, D., & Vacca, W. D. 1998, ApJ, 497, 618
Schaller, G., Schaerer, D., Meynet, G., & Maeder, A. 1992, A&AS, 96, 269
Schiavon, R. P., & Barbuy, B. 1999, ApJ, 510, 934
Slesnick, C. L., Hillenbrand, L. A., & Massey, P. 2002, ApJ, 576, 880
van den Bergh, S, 1973, ApJ, 183, L123
———. 2000, The Galaxies of the Local Group (Cambridge: Cambridge Univ. Press)
Vink, J. S., de Koter, A., & Lamers, H. J. G. L. M. 2001, A&A, 369, 574